Australian Government
Department of Defence
Defence Science and
Technology Organisation

Survivability of a Propellant Fire inside a Simulated Military Vehicle Crew Compartment: Part 2 - Hazard Mitigation Strategies and Their Effectiveness

Andrew H. Hart, Blair C. Lade and Garry R. Hale

Weapons and Countermeasures Division
Defence Science and Technology Organisation

DSTO-RR-0393

ABSTRACT

A number of combat vehicles carry their propelling charges and high explosive filled projectiles inside the crew compartment. Such arrangements give rise to questions about the prospects of crew survival in an unplanned munitions initiation event owing to co-habitation of the crew with an on-board magazine. DSTO has undertaken an experimental study to investigate this concern. As part of the trial described in *Part 1* of this report, the following hazard mitigation strategies were assessed for their effectiveness at reducing the thermal, ejecta and pressure threats posed to the crew by a range of propelling charge fire scenarios: two MIL-STD Automatic Fire Suppression configurations; personnel clothing configurations; and propelling charge storage tube confinement modification. Results from the study suggest that the prospects of crew survival could be improved by the implementation of one or more of the hazard mitigation strategies described within.

RELEASE LIMITATION

Approved for public release

Published by

Weapons and Countermeasures Division
DSTO Defence Science and Technology Organisation
PO Box 1500
Edinburgh South Australia 5111 Australia

Telephone: 1300 DEFENCE
Fax: (08) 7389 6567

AR-015-621
June 2013

APPROVED FOR PUBLIC RELEASE

Survivability of a Propellant Fire inside a Simulated Military Vehicle Crew Compartment: Part 2 - Hazard Mitigation Strategies and Their Effectiveness

Executive Summary

A number of combat vehicles carry their propelling charges and high explosive filled projectiles inside the crew compartment. To permit the provision of informed advice on future acquisition programs, the Capability Development Group tasked the Defence Science and Technology Organisation (DSTO) to investigate the prospects of crew survival in the event of an unplanned munitions initiation event owing to the co-habitation of the crew with an on-board magazine. After initial modelling work indicated that a propelling charge fire would indeed subject the crew to a hazardous and potentially life-threatening environment, a trial was conducted in mid-2010 to experimentally ascertain the survivability of the crew when exposed to such an event.

Part 1 of this report details the trials design and provides an assessment of the thermal, ejecta and pressure hazards posed to the crew for a range of propelling charge types and propelling charge module configurations. The results from this baseline study indicated that one or more of the thermal and ejecta environments created in the crew compartment from these propelling charge events would pose a life-threatening risk to the crew. *Part 2* addresses the effectiveness of the following hazard mitigation strategies at enhancing the prospects of crew survival: two different MIL-STD Automatic Fire Suppression (AFESS) configurations; personnel clothing configurations; and propelling charge storage tube confinement modification. In addition, experiments involving a number of different propelling charge ignition scenarios were conducted to investigate the hazards posed to the crew owing to inadvertent charge initiation at various stages of propelling charge handling in the crew compartment.

The present study suggests that the prospects of crew survival could be improved by the implementation of one or more of the hazard mitigation strategies detailed within. The results provided an insight into the mechanisms by which the AFESS is able to reduce the rate of, and in some cases the total, energy release from the propelling charge events; identified modification of storage tube confinement as a means of reducing hazards posed to the crew and postulates synergistic benefits if used in conjunction with an AFESS; and showed the judicious selection of clothing to afford increased thermal protection from skin burns.

This page is intentionally blank

Authors

Andrew H. Hart
Weapons and Countermeasures Division

Andrew Hart completed a Bachelor of Engineering (Chemical) degree at the University of Adelaide in 2001, attaining first class honours. Andrew commenced work for DSTO in 2002 as a member of Weapons Propulsion Group where his work initially focussed on R&D relating to cast-composite rocket motors. The emphasis of his work then shifted to gun propellants, and for the past 8 years he has been involved in a wide range of gun propellant related research activities in support of defence acquisition programs and is currently the DSTO S&T Advisor for JP2086 'Mulwala Redevelopment Project'.

Blair C. Lade
Weapons and Countermeasures Division

Blair Lade has been an instrumentation technician for over 40 years and been involved in the many aspects of instrumentation and data recording throughout his career. From earthquake, radiation and process monitoring through to live and studio sound recording, cinema engineering and photography, accuracy, reliability and repeatability have always been the driving forces.

For the last 13 years he has been the instrumentation officer at DSTO's static rocket motor firing site at Edinburgh South Australia and has developed and maintained the instrumentation systems and electronics for the site.

Garry R. Hale
Weapons and Countermeasures Division

Garry Hale completed an Associate Diploma in Electronic Systems Maintenance during his 20 years of service in the Royal Australian Navy. He has extensive experience in the support, maintenance, operation, and technical instruction of a variety of electronic systems. Including: missile control systems; gun control systems; Radar; Sonar; and, communications equipment. As such he is familiar with military procedures and requirements on exercise and in warlike operational zones. Since 2005 he has been working as a research assistant and technical officer for DSTO. He is currently studying a Bachelor of Science at the University of South Australia.

Contents

Nomenclature

AFESS	Automatic Fire Suppression System
ATC `	Alternative top zone propelling charge module
BCM	Bottom zone propelling charge module
BCS	Sodium Bicarbonate, $NaHCO_3$
FM200	1,1,1,2,3,3,3-Heptafluoropropane, C_3F_7H. Also called HFC-227ea.
HE	High explosive
HF	Hydrogen fluoride
HFS	Omega HS-4 heat flux sensor
LOAEL	Lowest Observable Adverse Effect Level
P	Pressure (kPa)
RH	Relative humidity
RHS	Rectangular Hollow Section
t	Time (s)
T1	Ambient room temperature, ceiling-height (K)
T2	Ambient room temperature, mid-height position (K)
T3	Ambient room temperature, floor-height position (K)
TCM	Top zone propelling charge module
v	Velocity (m/s)

This page is intentionally blank

1. Introduction

A number of combat vehicle platforms carry their propelling charges and high explosive (HE) filled projectiles inside the crew compartment.

To permit the provision of informed advice on future acquisition programs, the Capability Development Group tasked the Defence Science and Technology Organisation (DSTO) to investigate the prospects of crew survival in the event of an unplanned munitions initiation event owing to concerns about the co-habitation of the crew with an on-board magazine.

Conclusions from a baseline study [1] were that a combination of one or more of the thermal, ejecta and pressure environments created in the crew compartment from a single-storage tube propelling charge event creates an environment in which the potential for crew fatalities and the subsequent loss of the platform is high.

Table 1 summarises a number of possible hazard mitigation methods that may improve prospects for survival and that could be readily adapted to a proposed platform without adversely affecting platform operability and that would not incur a significant space penalty in what are, typically, volume-limited systems. The effectiveness of each of these hazard mitigation measures were assessed against a range of propelling charge configurations as part of the trial described in [1]. Results from the hazard mitigation study, which have provided an insight into possible benefits associated with each of these mitigation methods and an understanding of some of their governing mechanisms, are the subject of this paper.

Table 1: Potential hazard mitigation measures to enhance the likelihood of crew survival

Mitigation Method	Hazard
Clothing	Thermal
AFESS	Thermal
Storage Tube Modification	Thermal, ejecta, pressure

The use of protective curtains in armoured vehicles is also a potentially viable means of protecting personnel and other on-board munitions from thermal, ejecta and pressure threats. Whilst not assessed as part of the experimental trials program, this hazard mitigation strategy is addressed as a part of this paper with consideration given to its effectiveness against a threat analogous to that used in this trial.

2. Background

Two different propelling charge module types, representative of that used in particular armoured military vehicles, are considered in this paper: a top zone propelling charge module (TCM) and a bottom zone propelling charge module (BCM). Both propelling charge modules utilise a combustible case filled with propellant and a centre-core igniter train. The BCM and

TCM contain the same propellant formulation and centre-core ignition train design, but the propellant grain geometry and propellant mass is different for the two modules so that required ballistic performance and firing range profiles can be met. Each BCM weighs approximately 2.5 kg, of which 80% by mass is propellant. A single TCM weighs approximately 8.5 kg.

The layout of the hull of a representative armoured vehicle that was simulated in the trial is depicted in Figure 1. Propelling charge storage canisters run along the side walls of the hull, and HE filled projectiles also occupy the hull. The position of the single propelling charge storage tube represented in the trials structure is shown by the smaller of the two red outlines in Figure 1. A single propelling charge storage tube can hold up to 1xTCM or 3xBCM.

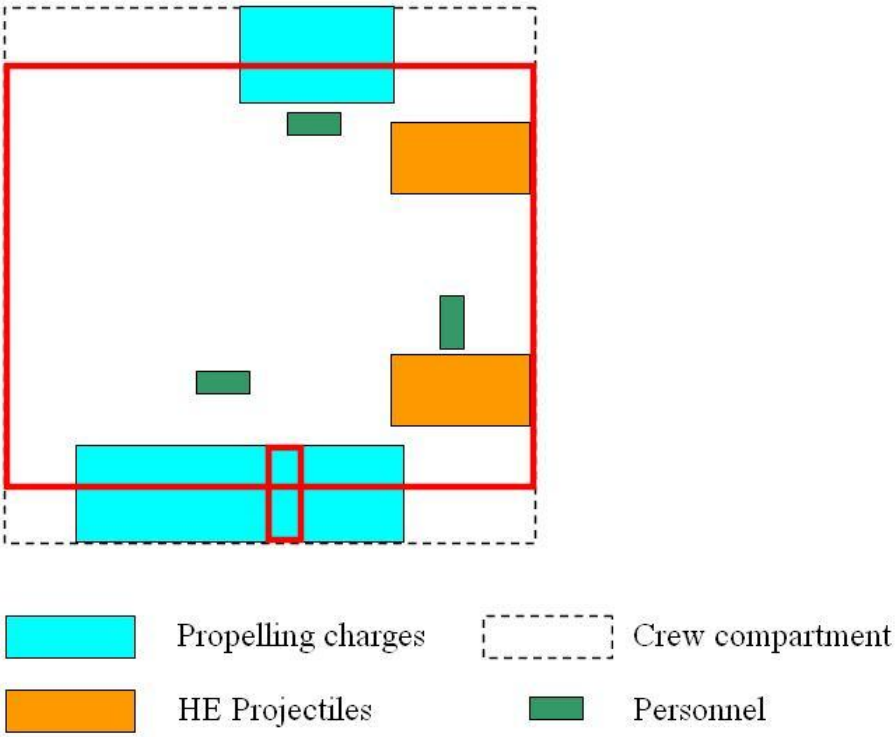

Figure 1: Cross-sectional area of crew compartment simulated in trial (larger red outline), hull ammunition storage locations, and position of the three simulated crew personnel. The position of the storage tube represented in the trial structure is shown with the smaller of the two red outlines.

It is assumed that the crew compartment is fitted with an Automatic Fire Suppression System (AFESS). Whilst such systems are almost universally employed in armoured vehicles, they are designed to combat fuel-fires rather than propelling charge events. Typically, the fire suppressant used is a fluorocarbon-based chemical that extinguishes fires via both chemical and physical means. Chemically, the suppressant reacts with intermediate combustion species (OH, O and H radicals) and halts chain branching reactions. Physical suppression occurs via temperature reduction and oxygen dilution. Chemical agents are unlikely to be effective against a propellant fire for two main reasons:

- The propellant contains both oxygen and fuel and therefore does not rely on atmospheric oxygen to combust.
- For a propellant fire occurring in a tube, the rate of gas generation and resultant momentum of the combustion gases will prevent a gaseous suppressant from reaching the burning surface, thus limiting the level of burning surface temperature suppression that can occur.

Effective fire suppression systems for propelling charge fires are predicated on rapid, directed quenching of the propellant surface by an agent that acts via physical means (heat absorption and cooling of the burning surface). Hence, water-based systems are preferred for such applications, and are most effective when the origin of the fire is well known as it permits a directed delivery of the water to the burning surface.

Whilst an AFESS tailored for fuel-fires is unlikely to have a significant effect on a burning propellant in a confined or partially confined state, the AFESS may provide sufficient temperature dilution to the crew compartment to prevent sympathetic cook-off and reduce the combustion intensity of unconfined propellant. Reference 2 provides more detail of available AFESS types and fire suppression agents, including their applicability, advantages and disadvantages, and their likely effectiveness against propelling charge events. Specific information regarding the AFESS assessed as a part of the trial is provided in Section 4.1.4.

To address the likelihood of crew survival during a propelling charge fire inside the crew compartment, the following hazards were considered the most relevant:

- Thermal environment
- Pressure environment
- Ejecta in the form of unburnt propellant grains, unconsumed modules and/or storage tube fragments and components
- Compartment toxicity.

The methods used to quantify the effects of these stimuli on the crew are described in Section 3.

3. Hazard Assessment

3.1 Thermal, Ejecta and Pressure

Skin burn damage was assessed using a one dimensional heat transfer model based on the work of Torvi and Dale [3] and Gasperin [4] to evaluate the temperature-time profile of the relevant skin layers at which second and third degree burns occur. In accordance with ISO 13506 [5], a first order Arrhenius rate proposed by Henriques and Moritz [6] was used to model the destruction rate of the skin.

Respiratory damage associated with the inhalation of hot gas is a significant hazard to the personnel inside the crew compartment in a propelling charge fire scenario. In full-scale fire tests of five residential dwellings undertaken to establish human tenability limits, Pryor [7] indicated that 149°C was a maximum temperature limit for escape in a dry environment. It was this value that was used to determine platform escape times from a respiratory damage perspective. In a saturated air environment, the maximum tolerable temperature drops to 70°C to 100°C [8,9].

Non-auditory overpressure effects on simulated personnel in the crew compartment were assessed using the injury prediction methodology developed by Axelsson and Yelverton [10] that is applicable to complex blast environments.

Ejecta related injury was assessed using a four parameter model developed from blunt force trauma data correlations by Clare *et al* [11].

Specific detail regarding the development and use of each of these hazard assessment methods is provided in *Part 1* of this report, see [1].

3.2 Compartment Toxicity

A propelling charge fire inside the crew compartment will create appreciable quantities of propellant combustion products, the main constituents of which are CO, CO_2, H_2, H_2O and N_2. All of these will displace and dilute the ambient oxygen concentration and species such as CO and CO_2 are toxic in their own right.

The AFESS agent used in the trial was the widely utilised 1,1,1,2,3,3,3-heptafluoropropane (FM200) with a small quantity of sodium bicarbonate (BCS) added (nominally 5% w/w). FM200 is non-toxic at low concentrations, but has a lowest observed adverse effect level (LOAEL) of 10.5% v/v [12,13]. For effective suppression of typical fire scenarios in confined spaces an 8-10% v/v concentration of FM200/BCS agent is suggested [14]. Given it is not possible to achieve completely homogenous dispersion of the suppressant throughout the volume of interest a typical design concentration for FM200/BCS is 12% v/v [15].

Of greater concern from a suppressant agent toxicity perspective, common to all fluorocarbon-based suppressants, is the production of the highly toxic hydrogen fluoride (HF) upon high temperature interaction between the suppressant and the flame. HF is produced by the high temperature thermal decomposition of fluorocarbons, and is also a by-product of the chemical reactions between the fluorocarbon and combustion radicals [14,16]. Hence, the level of acid gas production can be minimised by minimising the fire suppression time and thus extinguishing the fire before it becomes too large. This not only reduces the thermal severity of the event, but also limits the opportunity for HF producing reactions between the fluorocarbon and the intermediate combustion species.

The addition of acid product scavengers to fluorocarbon-based suppressants is a commonly employed technique to reduce HF levels. BCS is widely used in this role and is typically added at a 5% w/w level to the suppressant [17]. The BCS reduces the HF concentration in a

number of ways: the sodium ion is an effective flame inhibitor and the melting and subsequent decomposition of BCS is an endothermic process (+1626 kJ/kg). This reduces the concentration of the fluorocarbon needed to react with the flame to achieve effective suppression and also reduces flame temperatures, the propensity for re-ignition and extinguishment times. BCS also reduces the concentration of already formed HF via acid-base reactions. The incorporation of BCS to a fluorocarbon-based AFESS typically reduces HF concentrations by 50% [17]. However, it should be noted that such reductions rely on rapid extinguishment of the fire and the prevention of re-ignition. In a re-ignition scenario, the fluorocarbon suppressant is uniformly distributed throughout the room and much of the BCS powder may have adhered to surfaces within the room or dropped out of the air by the time that re-ignition occurs. This creates significant localised interaction between the flame and the fluorocarbon suppressant, but minimal interaction between the BCS and the flame, thus creating ideal conditions for HF production. To reduce the hazards associated with compartment toxicity, the incorporation of automatic compartment ventilation systems that operate shortly after AFESS discharge are commonly employed.

A summary of commonly used criteria for acid-gas exposure in occupied vehicle compartments is summarised in Table 2.

Table 2: Occupied vehicle acid-gas exposure criteria

Authority	Criteria (HF concentration)
US Army Surgeon General (Feb 1987)	<1000 ppm peak
Walter Reed (Sep 1989)	Delayed incapacitation: 746-2237 ppm-min over 5 min Immediate incapacitation: 1491-4473 ppm-min over 5 min
USMC EFV/AAAV (1999)	<1500 ppm TWA over 30 s <150 ppm TWA over 5 min

4. Experimental

4.1 Trials Structure

With the exception of the inclusion of the AFESS, the trials structure and deployed instrumentation are as described in [1]. For completeness, selected information from the aforementioned reference is repeated in sections 4.1.1 to 4.1.3.

4.1.1 Simulated Crew Compartment

The trials structure had internal dimensions of 3.3 m long x 2.3 m wide x 2.5 m high and was fabricated from 25 mm thick steel plate reinforced externally with lengths of Rectangular Hollow Section (RHS) and 350 grade 150 UB I-beams. Schematics of the trials structure are provided in Figure 2 and Figure 3. The location of camera viewing angles is described in Table 3, and the position of ambient room thermocouples are shown in Figure 3.

As described in [1], to overcome the predicted recoil forces acting on the propelling charge storage tube assembly during charge ignition, it was necessary to orientate the trials structure so that the storage tube was mounted on the floor (as opposed to being mounted horizontally on the side-wall of the platform, as is the case in reality). Hence, the trials structure internal geometry was designed to represent that of an actual platform lying on its side. This is illustrated in Figure 2.

4.1.2 Crew Personnel

Two lengths of 125x125x9 mm RHS traversing the width of the crew compartment were used to represent each of the three crew personnel (hereby denoted as Person A, Person B and Person C), see Figure 2, and 10 mm thick steel plate was bolted to both sides of the RHS between the head and groin positions. The instrumentation boards were bolted to the steel plates.

The width of the simulated personnel was 340 mm and the combined thickness of the lengths of RHS with the 10 mm thick plates on either side was 145 mm. A photograph of one of the simulated personnel (Person B) mounted inside the trials structure is shown in Figure 4. If the trials structure is considered in its correct orientation, that is, rotated on its side so that the propellant storage tube is on the side wall of the structure, the distance from the centre of the instrumentation boards representing the four body regions to the floor was as follows:

Groin	915 mm
Chest/Back	1315 mm
Head	1715 mm

The instrumentation boards were manufactured from synthetic resin bonded paper (SRBP). The SRBP was selected as it is: suitable for high temperature applications; is easy to machine; contains no silica based materials and so, unlike many other thermally insulating materials, will not be adversely affected by the presence of hydrogen fluoride (HF)[1]; and finally, the SRBP has a thermal diffusivity and a thermal effusivity similar to that of human skin. A photograph of an instrumentation board with all of its mounted instrumentation is shown in Figure 5.

[1] Created by the high temperature decomposition of fluorocarbon-based fire suppressants.

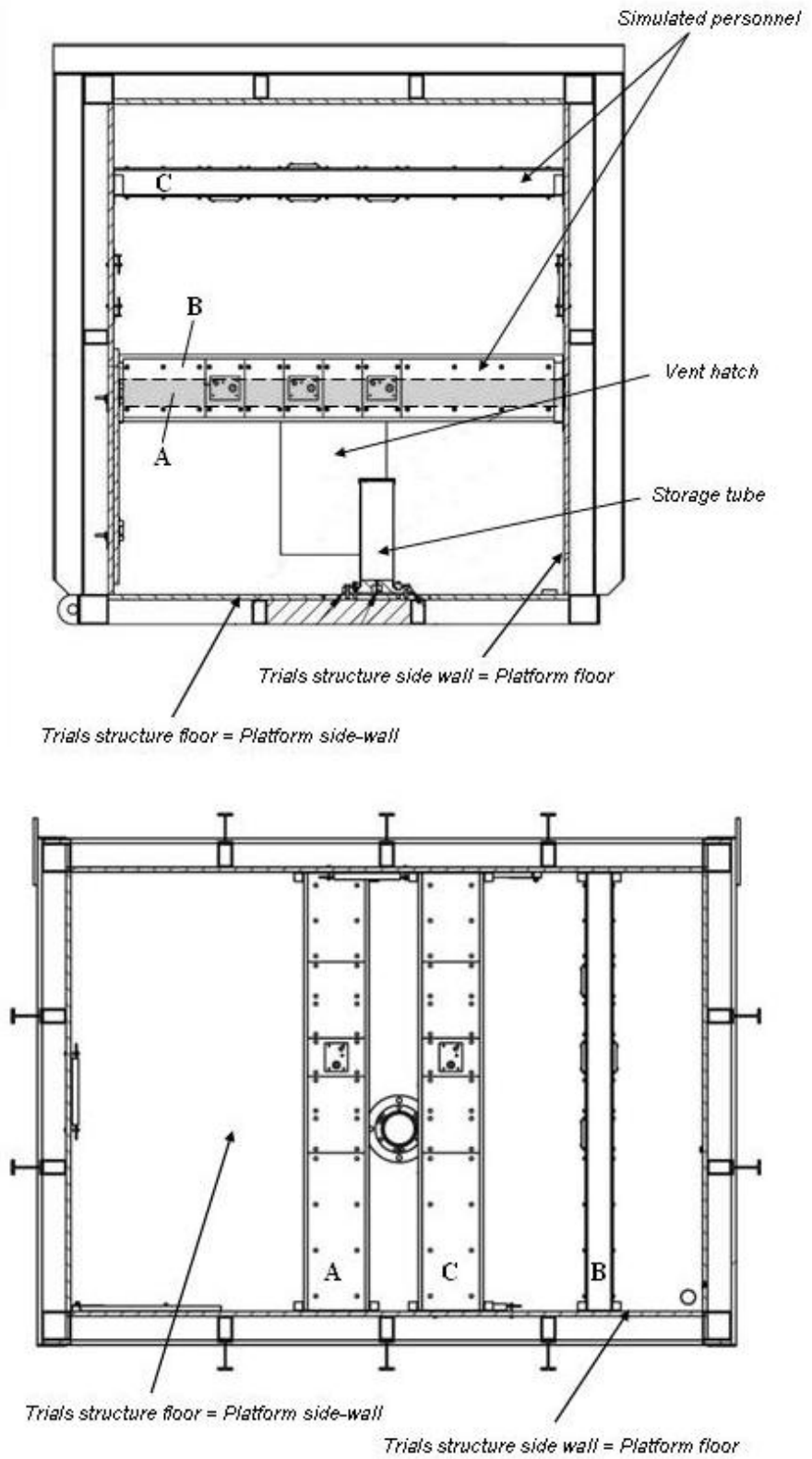

Figure 2: side-view (above) and top-view (below) schematics of the trials structure showing its orientation relative to the actual platform, The designation for each of the simulated personnel (Person A, B and C) is also shown.

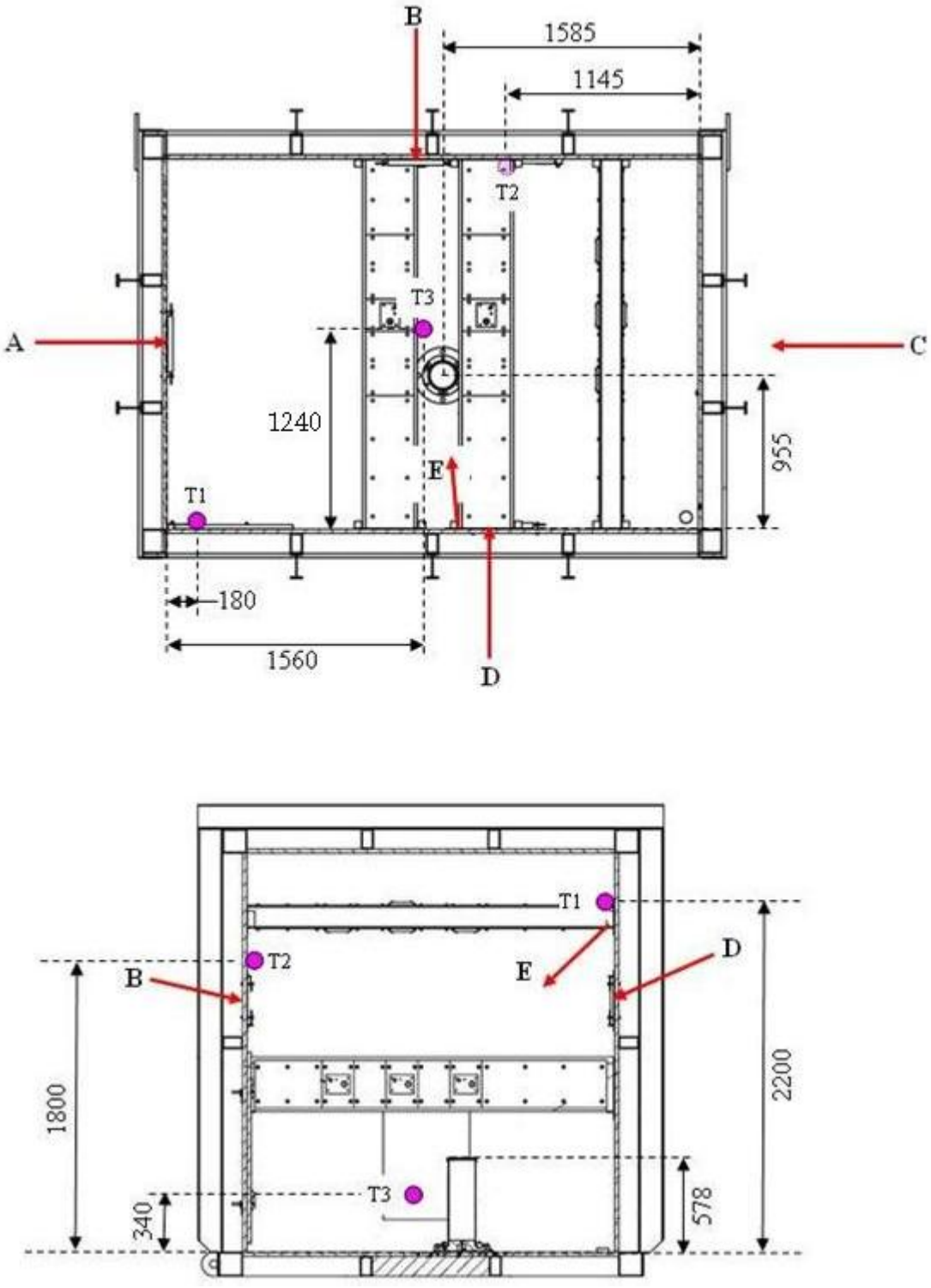

Figure 3: Approximate camera viewing angles (see Table 3) and position of the three ambient room thermocouples (dimensions in mm)

Table 3: Camera details

Experiment	View	Camera	Frame Rate/s	Record time (s)
1-2	A	Customised Cats Eye QC3495^	25	-
		Canon Exilim	420	600
	B	Canon Exilim	420	600
	C	KTK 801C or Cats Eye QC3495	25	-
	D	Photron SA1.1	3000	3.6
	E	KTK 801C or Cats Eye QC3495	25	-
3-15	A	Customised Cats Eye QC3495^	25	-
		Canon Exilim	420	600
	B	Mikrotron Cube 6	400	9
	C	Canon Exilim	420	600
		KTK 801C or Cats Eye QC3495	25	-
	D	Photron SA1.1	3000, 1000*	3.6, 10.9*
	E	KTK 801C or Cats Eye QC3495	25	-

^Cats Eye QC3495 sensor in a c-mount lens body with a Fujinon YV2.7x2.9LR4D2 lens set at 4 mm
*1000 fps was used for E7-E15

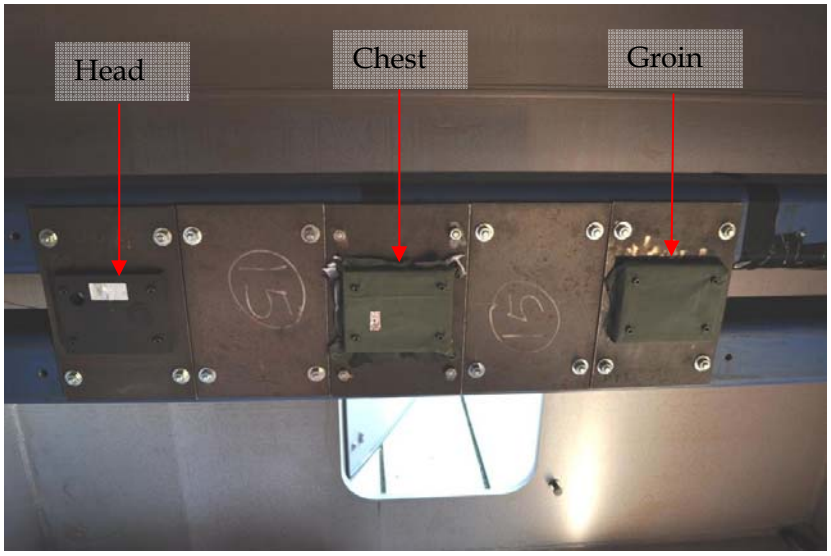

Figure 4: Photograph of the front of Person B with instrumentation boards and associated clothing

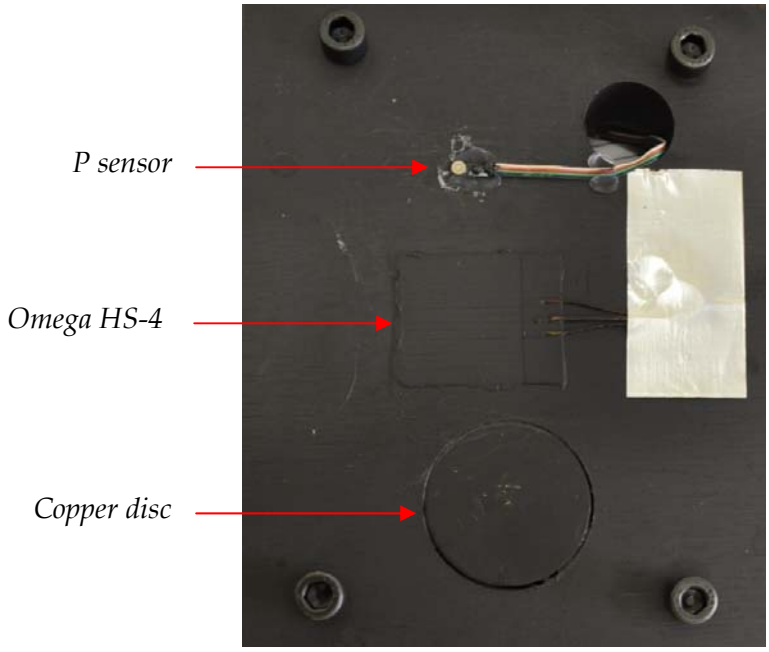

Figure 5: Instrumentation board with mounted sensors

The instrumentation boards representing the groin region were covered with a single layer of Nomex (93% meta-aramid, 5% para-aramid plain weave fire resistant cloth); the chest and back regions were covered by a single layer of cotton beneath a layer of Nomex to simulate the protection afforded to personnel wearing a t-shirt beneath their Nomex coveralls. The Nomex was selected on advice from the Defence Materiels Organisation (DMO) Combat Clothing Department [18].

4.1.3 Propelling Charge Storage Tubes

The propelling charge storage tubes were based on storage tubes used in platforms similar to that being represented in the trial and were designed to have an equivalent burst pressure.

The propelling charge storage tube was mounted on a 350 grade steel baseplate that was fitted with a centrally located PCB 111A23 pressure transducer. The baseplate was also machined with a slotted recess to house the igniter.

The propelling charges were initiated via a match-head that consisted of a 1 g SR371C filled silk bag attached to a Davey Bickford 2001 series electric igniter. To allow for base ignition, a 3 mm diameter hole was drilled into the side of the storage tubes at the same height as a cut-out channel in the baseplate so that the igniter lead could be fed out of the tube. After the igniter had been put in position, plasticine was used to seal any remaining flow area around the igniter wire and the drilled hole.

A polycarbonate disc, coupled with an end-cap retention ring was used in the trial, with finite element analysis used to determine the required polycarbonate thickness (6 mm) to replicate the confinement and failure mode of the storage tube end-cap being simulated.

4.1.4 Automatic Fire Suppression System (AFESS)

The AFESS used in the trial was based upon a crew compartment fire protection specification used in a comparable military platform to that being simulated in the trial. For the standard AFESS configuration testing performed in the trial, the AFESS consisted of:

- 2x Pacific Scientific ElectroKinteics Division Optical Fire Sensor Assemblies (P/N 25100003 Rev 1) conforming to MIL-PRF-6254B Sensor, Fire, Optical (Figure 6a).
- 1x Pacific Scientific HTL/KinTech Division AFESS Controller (Figure 6b), powered by two 12 V car batteries.
- 4x Class 3 extinguishers charged with FM200 and BCS, conforming to MIL-DTL-62547C(AT) (Figure 6c).
- 4x nozzles (Figure 6d)
- 4x customised extinguisher mounting brackets and installation cabling

The AFESS Optical Fire Sensor Assemblies, controller, nozzles and extinguishers were supplied, installed and operated over the course of the trial by Pacific Scientific HTL-Kin Tech Division, California, USA. The extinguisher mounting brackets and installation cabling was designed, fabricated and supplied by Cambridge Technologies, Melbourne, Australia.

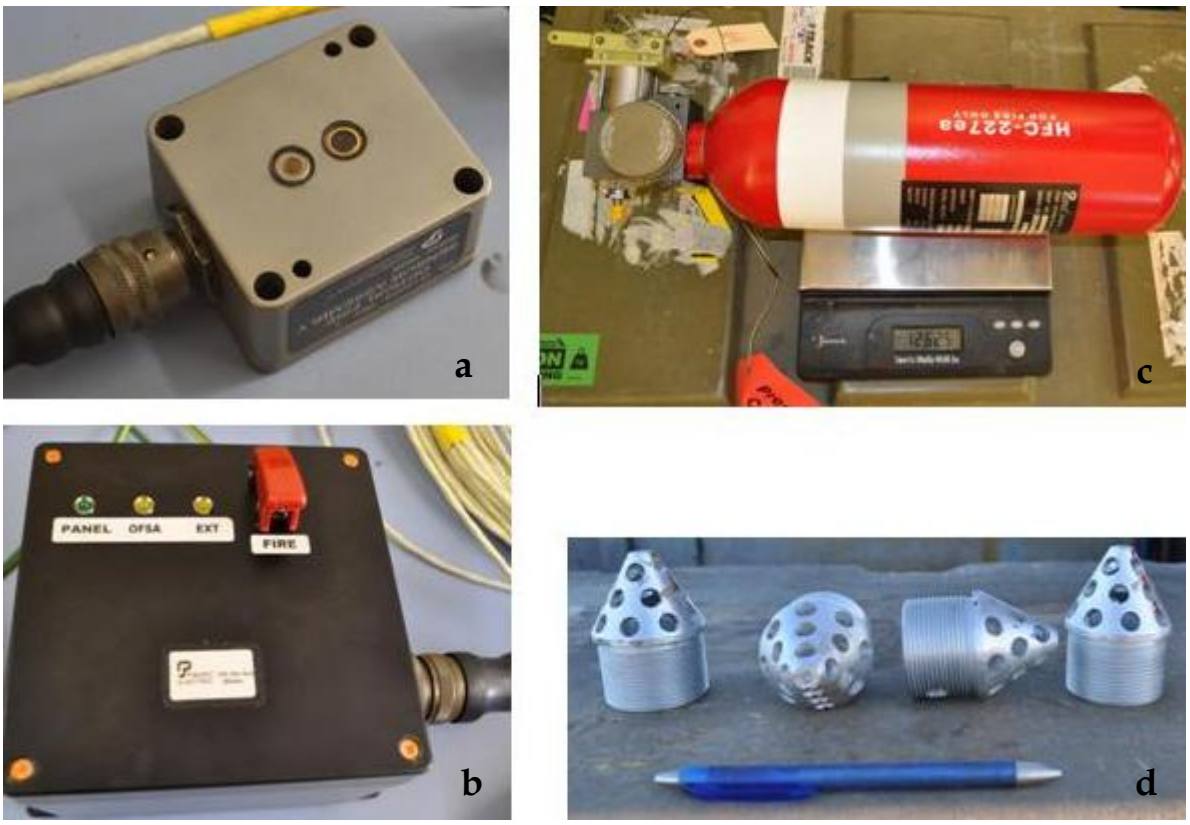

Figure 6: AFESS components

Based on the 19 m^3 internal volume of the trials structure, the quantity of FM200 contained in 4 x Class 3 bottles will give a suppressant concentration of 12% v/v inside the simulated crew compartment. This is the typical design concentration for FM200 that is used in an armoured vehicle AFESS [15].

As summarised in Section 4.3, five tests were conducted with the AFESS. For Experiment 13, the AFESS configuration was altered to include two water-filled extinguishers, each charged with approximately 3 kg of water and pressurised to 6.2 MPag with nitrogen, in addition to the four FM200+BCS filled extinguishers. For this configuration, as only four nozzles were provided, two of the FM200+BCS charged cylinders were fired without nozzles. The position of the key AFESS components is shown in Figure 7, the nozzle of the extinguishers were approximately 1380 mm above the floor.

Figure 8 is a photo of the trials structure prior to conducting Experiment 6 that shows three of the four FM200+BCS extinguishers. Also visible in the photo is one of the optical detectors (*circled*), the plywood vent hatch (*bottom centre of photo*), Person B (*partly obscured by access door*), Person C (*top of photo*), the back of Person A and the ambient room temperature thermocouple *T2* (*arrow*).

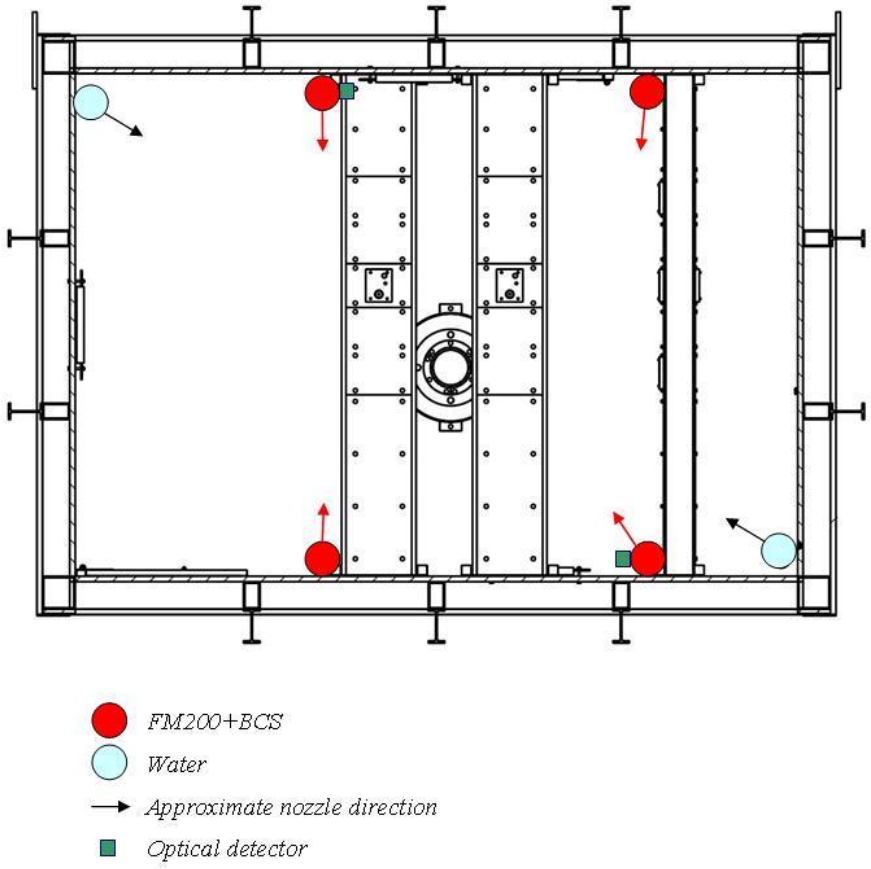

Figure 7: Position and direction of the AFESS extinguishers and optical detectors in the trials structure

Figure 8: Photo of the trials setup prior to conducting Experiment 6

Figure 9 is a photo of the extinguisher configuration on one side of the trial structure showing two of the four FM200+BCS extinguishers for Experiment 13. For this experiment, two of the gas-filled extinguishers were fired without nozzles, one of which is visible in the figure (*circled*). One of the two water-filled extinguishers (*arrow*) is also visible. A portion of the plastic flash bulb reflector can be seen in the top left hand side of the photo.

Open-air extinguisher testing was conducted to determine solenoid valve opening times, agent discharge velocities and suppressant discharge pattern. These parameters were determined from two high speed cameras: a Photron APX-RS positioned at right angles to the nozzle shooting at 1000 frames/s; and a Photron SA1.1 positioned end-on to the nozzle, shooting at a frame rate of 2000 frames/s. Suppressant discharge temperature was measured with a K-type thermocouple positioned approximately 10 mm downstream from the nozzle. The following extinguisher configurations were tested:

- FM200+BCS charged extinguisher with nozzle
- FM200+BCS charged extinguisher without nozzle
- Water charged extinguisher with nozzle

Results from these open-air tests are summarised in Section 5.4.1.

Figure 9: Extinguisher configuration on one side of the trials structure for the combined water and gaseous suppressant experiment (Experiment 13)

4.2 Instrumentation

4.2.1 Thermal

Heat flux was measured using two types of sensors: Omega HS-4 thermopile sensors, from Omega Industries, that give a direct measure of heat flux as well as temperature; and a combination of 1.6 mm and 1.2 mm thick, 35 mm diameter copper discs (>99% purity) whose temperature was measured with a K-type thermocouple attached to the centre of the back face of the disc with a small bead of 60/40 Pb/Sn solder (melting point of 190 °C). The exposed face of the Omega HS-4 gauges and copper discs were painted with matt black Septone Heat Proof paint to give a sensor emissivity close to that of human skin, ε=0.94 [19].

Both the Omega HS-4 gauges and the K-type thermocouples attached to the copper discs were sampled at 100 Hz and the data was then filtered at 10 Hz.

A lumped heat capacity analysis was used to convert the transient temperature profile of the copper discs to a heat flux that could then be used for burn damage calculations. A detailed description of the heat flux instrumentation development and applied data reduction procedures are provided in [1].

In addition to the heat flux and temperature measurements on the simulated personnel inside the crew compartment, three K-type thermocouples were positioned inside the crew compartment to monitor the ambient temperature profile. The location of these thermocouples

is shown in Figure 3. The K-type thermocouples were sampled at 100 Hz. Custom designed thermocouple modules, described in [1], were used to permit accurate temperature measurements at these sampling rates.

The ambient temperature and relative humidity (*RH*) was measured inside the simulated crew compartment immediately prior to each experiment using a PCWI whirling hygrometer. All ambient crew compartment temperature data presented in the report is normalised to a starting environmental condition of 15 °C and 65% *RH* at an atmospheric pressure of 101 kPa.

4.2.2 Ejecta

A range of cameras were used from different viewing angles to allow ejecta velocities and dispersion to be measured and observed. Camera operational details and viewing angles are summarised in Table 3 and Figure 3 respectively.

To provide illumination for the initial stages of the propelling charge event two PF330 flash bulbs of 1 s burn duration were used in conjunction with consumable plastic flash bulb reflectors mounted at the ceiling above the viewing angle A window.

Ejecta velocities were determined from images captured from viewing angles B and D using a Photron SA1.1 camera and a Mikrotron Cube 6 camera. Both cameras were fitted with Nikon 17-35 mm lenses.

To assess the distribution of ejecta from the storage tube, for selected experiments a 1 mm thick aluminium witness plate, with a cross-sectional dimension of approximately 1.2 m by 0.9 m, was mounted on the ceiling of the crew compartment with an 8 mm standoff distance. The witness plate was positioned directly above the propelling charge storage tube with the bottom and top of the witness plate extending past the groin and head of Person C respectively.

4.2.3 Pressure

Four Kulite LE-080-250PSIA thin line, high temperature pressure transducers were attached to the chest, back and sides of Person A, B and C to measure the dynamic pressure experienced by the thorax of the crew. The thin profile of these sensors meant that protrusion above the level of the clothed instrumentation board was minimal. To remove any possible influence of the clothing on the measured pressures, as recommended in [20], a small hole was cut in the fabric swatches so that the transducer would not be covered by clothing. To prevent any flame or gas migration into the hole cut in the fabric swatches, the fabric around the transducer was taped to the instrumentation board with a small piece of aluminium tape.

The pressure transducers were sampled at 100 kHz.

4.2.4 Compartment Toxicity

Because platforms of the type being simulated in the trial commonly use automatic ventilation systems, the threat posed to crew survival by compartment toxicity was assumed secondary

relative to the immediate thermal, pressure and ejecta threats that could be created in a propelling charge event. As such, *in-situ* real-time monitoring of the atmosphere within the trials structure was not performed during the trial.

To ensure the safety of the trials participants, after the conduct of an experiment a number of measures were put in place prior to personnel being permitted entry into the trials structure.

For baseline experiments, the camera footage fed to the control bunker was used for a preliminary post-test clearance check. Following this, the clearance officer opened the trials structure access doors and turned on a blower positioned at one of the doors to ventilate the structure. An Eagle meter gas detector was also available to measure the atmospheric oxygen content inside the trial structure.

For experiments involving the AFESS, stringent HF protection measures were employed that involved atmospheric HF measurements using HF selective Drager tubes and a Drager pump as well as trials structure and personnel decontamination after each experiment. This is discussed in detail in Appendix B.

4.3 Trials Schedule

Results from the baseline experiments of Table 4 are provided in [1]. The experiments listed in Table 5 were undertaken to assess the effect of storage tube modification, propelling charge ignition location and use of an AFESS on the hazards posed to the crew in a single propelling charge storage tube event. Results from the experiments listed in Table 5 are the subject of this paper.

Table 4: Baseline experimental schedule

Experiment	Module	Confinement
1	2xBCM	Hatch
2	3xBCM	Hatch
3	1xTCM	Outer Plywood
4	2xBCM	Outer Plywood
9	2xATC	Outer Plywood
10	3xBCM	Outer Plywood
14	3xBCM	Inner Plywood

Table 5: Hazard mitigation experimental schedule

Experiment	Module	Other
Storage tube modification and ignition location		
11	3xBCM	No end-cap
12	3xBCM	No end-cap, top ignition
15	3xBCM	Loose modules
AFESS experiments		
5	2xBCM	4xGas
6	1xTCM	4xGas
7	3xBCM	4xGas
8	2xBCM	4xGas
13	1xTCM	4xGas + 2xWater

All AFESS experiments were conducted with a storage tube end-cap in position, base ignition and with a sheet of plywood mounted on the outside of the crew compartment vent hatch. Experiment 8 was a repeat of Experiment 5 and was conducted to assess the repeatability of the AFESS performance.

5. Results and Discussion

5.1 Event Sequence

The sequence of events from match-head ignition through to the completion of propelling charge combustion were investigated for each experiment using the array of cameras deployed in and around the trials structure. Points of interest noted from this footage are summarised in Section 5.1.1 to 5.1.4. Times quoted refer to the time elapsed after the firing pulse was sent to the match-head. For view angles A and E, the cameras used were only time stamped to the nearest second. Hence, whilst the described images for these view angles are placed in chronological order, a more precise time for the presented frames can not be provided. The reader is referred to Table 3 in Section 4.2.2 for a description of the camera detail and orientation for the view angles quoted in this section.

5.1.1 3xBCM Baseline

Complete event sequences for the 3xBCM configurations were not able to be determined due to: image obscuration associated with module flash suppressant and ejecta dispersion shortly after end-cap failure; and, image saturation due to the intensity of the fire inside the trials structure. A summary of the events noted for Experiment 10 are provided in Table 6, with selected images provided in Figure 10.

Table 6: Sequence of events for 3xBCM baseline configuration, Experiment 10, as noted from camera footage. See Figure 10 for selected images.

View Angle (Image)	Time (ms)	Observation
D	236	Evidence of match-head output
D (1)	323	Storage tube end-cap failure
D (2)	328-333	Debris and ejecta exits tube
-	360 ms	Vent hatch opens
-	333-402	Complete image obscuration
D	402	Orange glow on image indicates fire development
D	435	Propellant grains and centre-core igniter material can be seen moving towards the roof
D	464-1474	Image appears black
D	1474	Orange glow on image indicates fire development
D	2000	Mass fire developed
B (3)	3294	Person A and C (*arrows*) subjected to high intensity flame impingement.
B	3300	Clothing of chest and groin of Person C on fire
D	3976	Fire begins to reduce in size
D	4534	Bulk fire in room ceases, localised portions of propellant continue to burn on ground.
D	4600-5880	Low intensity combustion continues in tube
A	~9 000	Combustion ceases

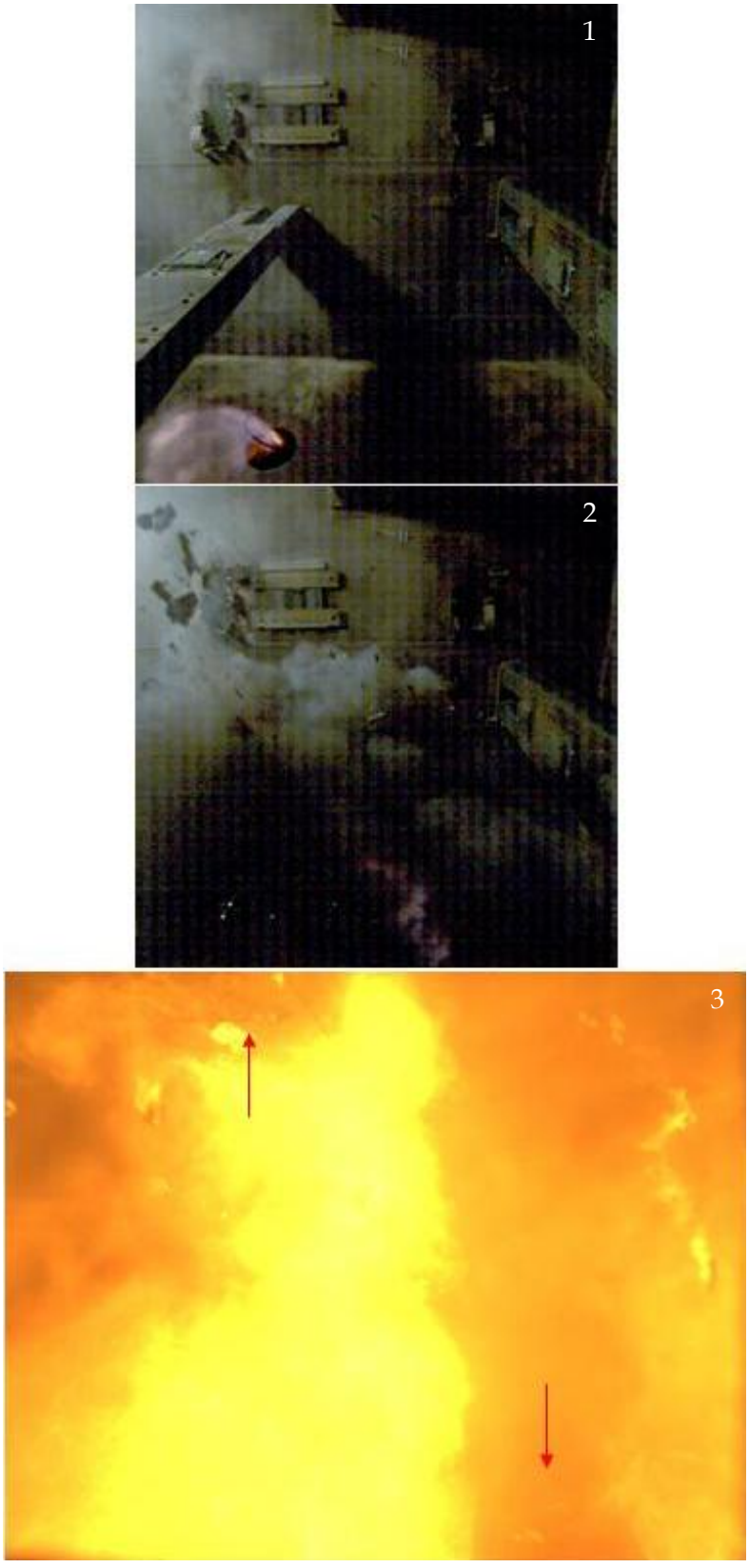

Figure 10: Selected images for Experiment 10, refer to Table 6.

5.1.2 3xBCM No End-cap

Base ignition of a 3xBCM configuration in the propelling charge storage tube, without an end-cap fitted (Experiment 11), was performed to assess the effect of reduced tube confinement on the thermal, pressure and ejecta hazards posed to the crew.

Three hundred and sixty grams of unburnt propellant was collected after Experiment 11, and a number of areas where the unburnt grains were concentrated are circled in Figure 11. The burn marks on the floor of the trials structure suggest that combustion regions were less disparate in the absence of the end-cap when compared with configurations tested with an end-cap (see for example Section 5.1 of [1]). This is discussed further in Section 5.2.1.

Figure 11: Burn marks suggesting a reduced dispersion of combustion zones in the absence of a storage tube end-cap. Locations of unburnt propellant grains are circled.

Table 7 summarises the sequence of events for Experiment 11. Selected images, denoted in brackets in the table, are provided in Figure 12.

Table 7: Sequence of events for base ignition of a 3xBCM configuration without a storage tube end-cap, Experiment 11, as noted from camera footage. See Figure 12 for selected images.

View Angle (Image)	Time (ms)	Observation
D	72	Evidence of match-head output
D	146	Match-head sparks exiting the tube through the annular gap between the modules and the tube
D (1)	187-473	Flame from match-head exiting tube through the module/tube annular gap
D	523	Black smoke coming through module/tube annular gap
D	646	Three modules start exiting tube as one
D	654	Modules continue to be lifted out of tube by pressure at the base
D	663	Fire/gas release as bottom module exits tube
D (2)	705	Base of lower module partially separated and propellant falling out of lower module
D (3)	841	Large fire from initial ignition event emanating from tube
D (4)	1026	Piece of burning combustible case and propellant grains falling from ceiling
B (5)	1045	Modules falling back to ground (see arrows), base of upper module separated, large portion of upper module propellant grains 'sitting' on top of middle module.
B (6,7)	1093-1147	High momentum gas jet from middle module centre-core develops followed by gas jet ignition and subsequent fireball from either end of the attached middle and lower modules
D	1235	Unburnt grains falling to floor
B	1309	Shell of upper module combustible case bounces off Person A, the other two modules drop between Person A and Person B.
B (8)	1616	Firebrands/burning material falling from roof
D (9)	2290	Fire from module and propellant grains develops beneath Person B.
D (10)	3953	Jetting flame from module centre-core in bottom RHS of frame flowing over unburnt grains on ground.
D	4533	Vent hatch opens
A (11)	~10 000	Escalation of fire between Person A and B
A (12)	~16 000	'Roman candle' effect from storage tube
A	~40 000	Propellant combustion ceases

Figure 12: Selected images for Experiment 11, refer to Table 7

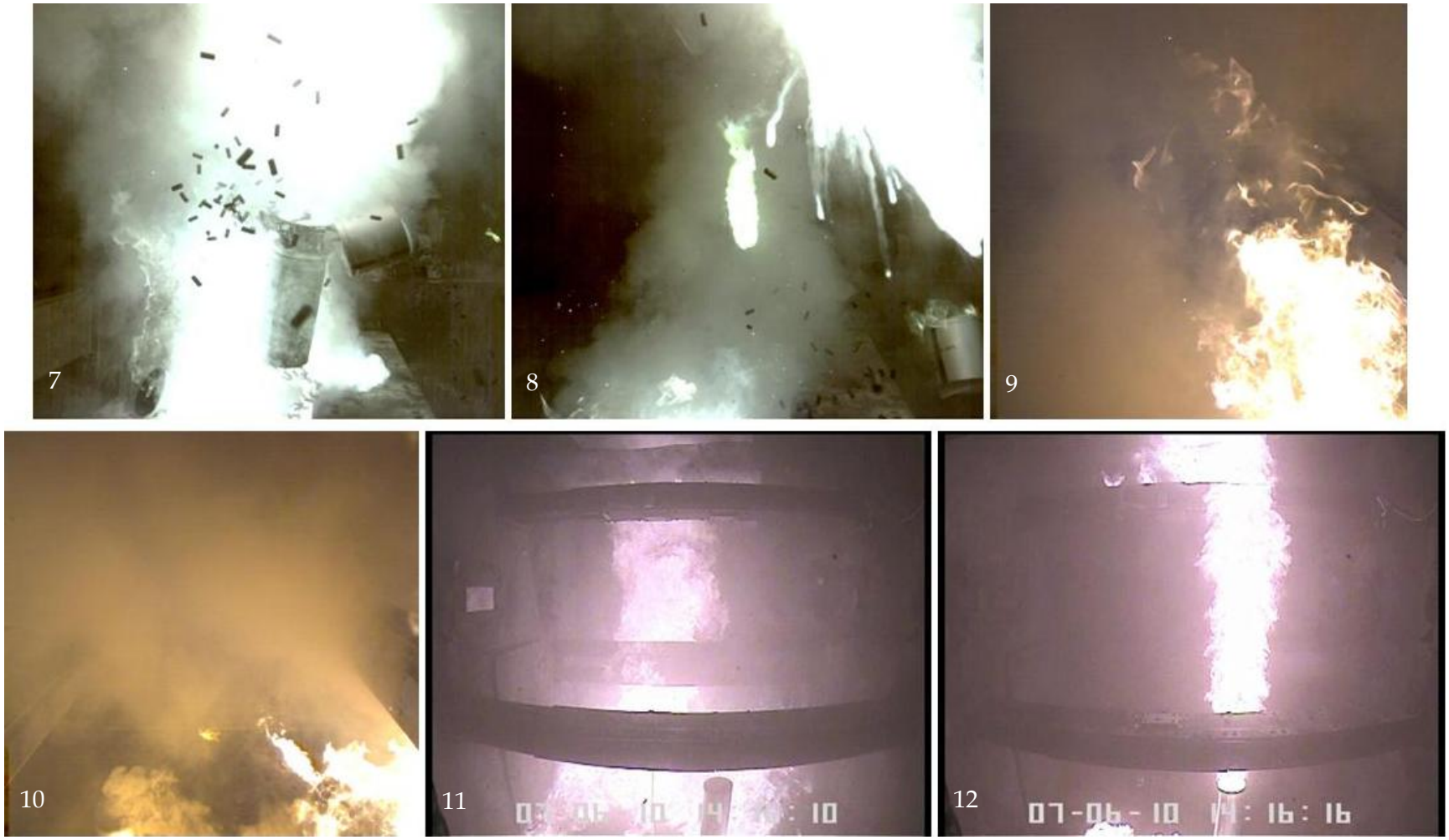

Figure 12: Selected images for Experiment 11, refer to Table 7 (cont.)

5.1.3 3xBCM No End-cap, Top Ignition

The ignition of a 3xBCM configuration via a match-head taped to the top of the upper module, without an end-cap on the storage tube (Experiment 12), was conducted to represent inadvertent propelling charge initiation from the inside of the crew compartment. Examples of scenarios that could cause such an event would be charge initiation via hot ash from a cigarette, or a small fire inside the crew compartment initiating a charge inside a non-sealed storage tube.

Figure 13 provides an example of burn damage sustained by the chest and groin of Person A and B respectively. For this experiment, the chest of Person A sustained 3rd degree burns after 29 s and the groin of Person B sustained 3rd degree burns after 15 s exposure.

Figure 13: Burn damage sustained by the clothing of Person B groin and Person A chest for Experiment 12

Table 8 summarises the sequence of events for Experiment 12. Selected images, denoted in brackets in the table, are provided in Figure 14.

Table 8: Sequence of events for 3xBCM configuration with top ignition, Experiment 12, as noted from camera footage. See Figure 14 for selected images.

View Angle (Image)	Time (ms)	Observation
E (1)	0	Module setup
D	9	Evidence of match-head output
D (2)	26	Match-head output
D	107	Ignition of upper module centre-core igniter material
D (3)	298-463	High momentum gas jet and flame from upper module centre-core.
D	473	Upper module centre-core gas momentum decreases
D (4)	744	Gas jet and flame develops from middle module centre-core
D	742	Upper module starts to lift from tube
D	785	Upper module rises out of tube, allowing accumulated gas and flame from below the module to escape tube.
D (5)	869	As upper module travels up the screen, flame predominately emanates from centre-core (*arrow*). Bulk of module not burning.
D	1202	Burning of middle module centre-core starts to lose intensity
D (6)	1219	Middle module lifts from tube (*arrow*)
B (7)	1222	Upper module strikes ceiling, middle module exiting tube
B	1340	Collision between upper and middle modules
D (8)	1983	Upper and middle module combustible cases start to burn
B	2044	Upper module bounces off Person A, middle module comes to rest next to storage tube.
D (9)	3216	Propellant combustion develops in storage tube
D	3382	Vent hatch opens as evidenced by uniform, sudden change in gas flow direction inside trials structure.
B (10)	3814	Lower module exits tube with little momentum and rotating through the air ejects both unburning and burning grains
B	4040	Grains burning in mid-air after being ejected from lower module.
E	-	Lower module comes to rest sideways on top of storage tube and starts burning.
E	-	Lower module combustible case loses structural integrity and peels open.
B (11)	5068	Mass fire developed
B (12)	6790	Localised, high intensity flame impingement on Person C groin.
A	~20000	Propellant combustion ceases

Figure 14: Selected images from Experiment 12, refer to Table 8.

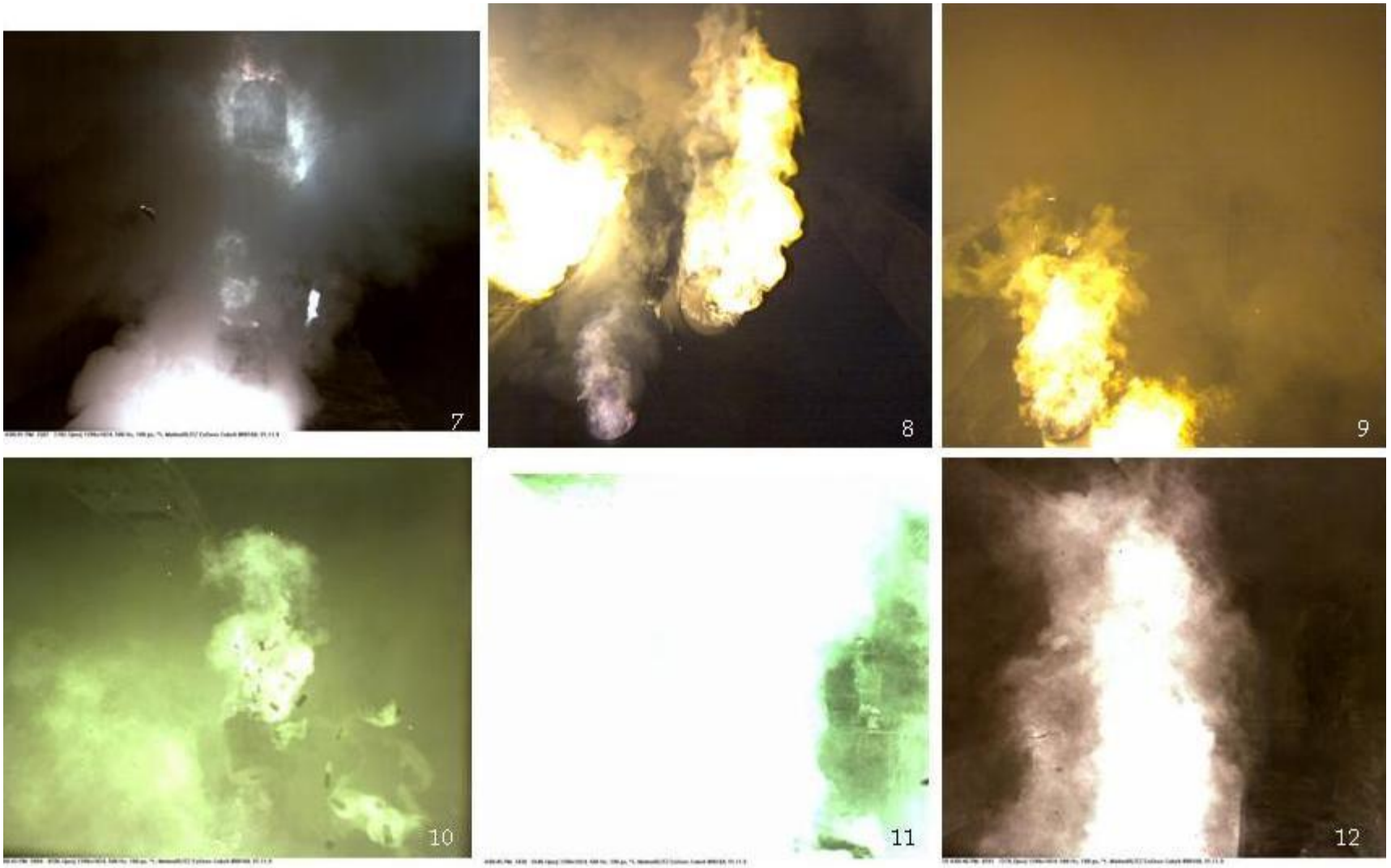

Figure 14: Selected images from Experiment 12, refer to Table 8 (cont.)

5.1.4 3x BCM Loose Module Configuration

The loose module configuration was tested to assess the likely effect of a 3xBCM event during a firing operation where modules may be sitting on the crew compartment floor waiting to be loaded. To simulate this, 3xBCMs were positioned atop the baseplate. No storage tube was used and the 3xBCM configuration was base-ignited.

Table 9 summarises the sequence of events for Experiment 15. Selected images, denoted in brackets in the table, are provided in Figure 15.

Table 9: Sequence of events for 3xBCM loose module configuration, Experiment 15, as noted from camera footage. See Figure 15 for selected images.

View Angle (Image)	Time (ms)	Observation
E (1)	0	Module setup
D	16	Evidence of match-head output
D	634	Visible lifting of modules off baseplate
E (2)	~700	Accumulated fire/gas from between base of module and baseplate escaping
D,E	795	Gas production from upper module centre-core first evident. Upper module separates from bottom two modules.
D (3)	873	Gas production from upper module centre-core
D	937	Upper module centre-core ignition
D (4)	1013	Jet of fire from upper module centre-core
A (5)	~1200	Bulk ignition of centre-core igniter material from other modules
E (6)	2720	Bottom two modules rolling towards Person B, upper module rolling beneath Person A.
D	3160	Propellant grains from module near Person A 'spitting' out of module with low momentum
A	3605	Vent hatch opens
A	4131	Mass fire develops
E	~6300	Base of one of the modules next to Person B blows off projecting module contents and propellant against the side wall of the trials structure with high momentum
E (7)	~6800	Image of propellant from a module scattered below Person B prior to combusting (RHS of image)
D (8), A (9)	~7900	Residual propellant scattered around Person B creating 'Roman candle' effect
D	10700	Cessation of burning in trials structure

Figure 15: Selected images from Experiment 15, refer to Table 9.

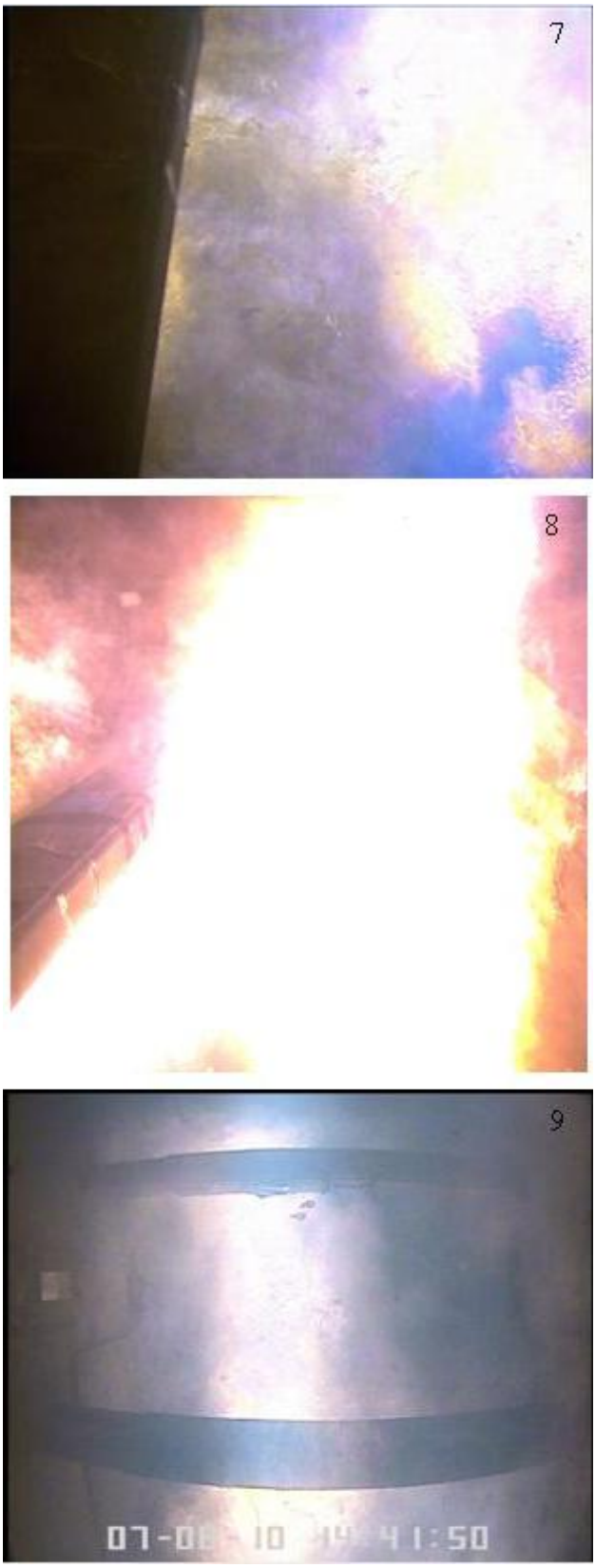

Figure 15: Selected images from Experiment 15, refer to Table 9 (cont.)

5.2 Storage Tube Modification and Ignition Location

5.2.1 Thermal

This section addresses the thermal hazards posed to the crew from the experiments conducted without the AFESS. AFESS results are presented and discussed in Section 5.4.

Burn charts are provided in this section as a means of summarising the burns sustained by the three personnel inside the simulated crew compartment, and are provided for two scenarios:

- Crew personnel exposed to the thermal environment inside the crew compartment for 10 s. This was considered a realistic time for all of the personnel inside the crew compartment to escape if they have not sustained any injuries that affect their mobility or their ability to operate latches to escape hatches or the rear access door.

- Crew personnel exposed to the thermal environment for 30 s. This was assumed to be representative of a scenario where the crew were unable to immediately escape the vehicle due to injuries that may have been sustained, or if the propelling charge event affected the structure of the crew compartment in such a way that egress from the crew compartment was not initially possible.

Burn injuries for these two scenarios were modelled by applying the measured transient heat fluxes for either 10 s or 30 s. After this time the heat flux was set to zero and so any additional burning sustained after this time is as a result of burns occurring as the skin cools. Integrating the heat flux versus time curves gives the energy absorbed and these values are presented for a 10 s exposure time as an additional comparative tool.

Ambient crew compartment temperature conditions are plotted versus time to permit an assessment of escape time from a respiratory viewpoint, and to consider the likelihood of sympathetic cook-off of munitions stored in the crew compartment. The plotted temperature is the average of thermocouples *T1* and *T2*, see Figure 3 in Section 4.2.1, as these thermocouples were positioned at approximately head height and are therefore of most relevance from a respiratory hazard perspective. The vertical dashed lines in these plots correspond to the time of vent hatch failure.

It should be noted that the measured crew compartment temperatures and heat fluxes are not only influenced by the experimental variable of interest, but also by the gas dynamics inside the room, both prior to and upon room venting, and where propelling charge modules and propellant gets distributed over the course of the event. Post experiment inspection and video footage was used where possible to track the distribution of propellant and propelling charge modules for each experiment, and where relevant, these are commented upon in light of the observed results.

The burn chart and 10 s exposure energy absorption plots presented in Table 10 and Figure 16 respectively show that, with the exception of the base-ignited, no end-cap configuration of Experiment 11, the 10 s burn levels will almost certainly cause fatal skin burns for Person A and C. The maximum escape times are shown in Figure 17 and range from 3.7 s for the

baseline configuration to 6.8 s for Experiment 11 where both the rate of energy release and the total energy release was lowest.

The difference in energy absorption levels and ambient crew compartment temperature conditions for the four events considered in this section stems from four, interrelated variables: initial module ignition development; rate of energy release; total energy release; and the spatial uniformity of propellant/module burning inside the crew compartment. These parameters are described in detail in [1].

Initial ignition development for the baseline configuration was highest owing to the confinement afforded by the use of an end-cap creating higher pressures and therefore higher initial igniter material burning rates.

Reference [1] demonstrated the importance of the rate of energy release as a thermal hazard determining factor. If the energy from the propelling charge event was liberated uniformly throughout the crew compartment, then the average rate of energy release data presented below would predict a thermal threat increasing in the order:

E11 {energy release=739 kJ/s} << *E12 {1557 kJ/s}* << *E15 {2911 kJ/s}* < *E10 {3461 kJ/s}*

However, inspection of the data presented in Table 10, Figure 16 and Figure 17 shows that the thermal threat for Experiment 12 was of a similar severity to that posed by Experiment 15. In the absence of an end-cap, initial charge ignition development is reduced and the acceleration afforded to modules/propellant upon tube depressurisation at the time of end-cap failure is no longer present. As a consequence the nature of the subsequent ejecta is affected: for the 3xBCM baseline configuration (Experiment 10), the majority of ejecta was in the form of high velocity propellant grains that, once ejected from the storage tube, were evenly distributed across the floor of the trials structure prior to combusting; in the absence of an end-cap, propelling charge modules exited the tube whole and with low velocity. In this latter case, the bulk of the energy release is from a smaller number of spatially concentrated areas in the trials structure. As a consequence, the level of burn damage sustained by personnel is also influenced by the position where the propelling charge modules come to rest once they have been ejected from the storage tube.

If all parameters other than the dispersion of propellant are equal, it takes less time for combustion to propagate from burning material to unburnt propellant grains if all of the combustible material is in close proximity. Whilst the propellant dispersion is the most widespread for the baseline case, thus ordinarily slowing the rate of energy release, this is compensated for by the enhanced charge ignition development associated with the presence of an end-cap, coupled with the generation of significant quantities of additional propellant surface area through grain fracture upon impact with the surfaces inside the crew compartment.

Table 10: Burn charts for 3xBCM configurations tested under different module storage and ignition point conditions at (a) 10 s personnel exposure, (b) 30 s personnel exposure

(a) 10 s exposure		**Person A**				**Person B**				**Person C**			
Storage	Experiment	Groin	Chest	Back	Head	Groin	Chest	Back	Head	Groin	Chest	Back	Head
baseline	10	3,16	9	8	2,10	4	9	-	2,10	1,<7[n]	3,10	-	3,12
no end cap	11	10	-	-	8	8	-	-	8	10	-	-	7
top ignition	12	5,16	10	9	5,<17[F]	5,15	-	-	5,14	5,20	8	10	5,13
loose	15	5,14	8	-	4,<11[i]	5,20	-	-	5,11	7	No data[b]	-	5,12

(b) 30 s exposure		**Person A**				**Person B**				**Person C**			
Storage	Experiment	Groin	Chest	Back	Head	Groin	Chest	Back	Head	Groin	Chest	Back	Head
baseline	10	3,16	9	8	2,10	4,28	11	18	2,10	1,<7[n]	3,10	14	3,12
no end cap	11	10	29	-	8	8	16	14	8,21	10,39	18	17	7,32
top ignition	12	5,15	10,29	9,35	5,<17[F]	5,15	12	14	5,14	5,16	8,27	10	5,13
loose	15	5,14	8,40	12	4,<11[i]	5,17	14	19	5,<11[K]	7,26	No data[b]	17	5,<12[m]

a,b	3rd degree burn, a=time to 2nd degree burn (s), b=time to 3rd degree burn (s)
a	2nd degree burn, a=time to 2nd degree burn (s)
a	1st degree burn, a=time to first degree burn (s)
-	No burn sustained

[b]Faulty sensor

[n]Cu disc failed at 3.5s at 150°C

[F]Cu disc failed at 8.0 s at 105°C

[i]Cu disc failed at 8.4s at 190°C

[K]Cu disc failed at 10.1s at 189°C

[m]Cu disc failed at 10.3 s at 185°C

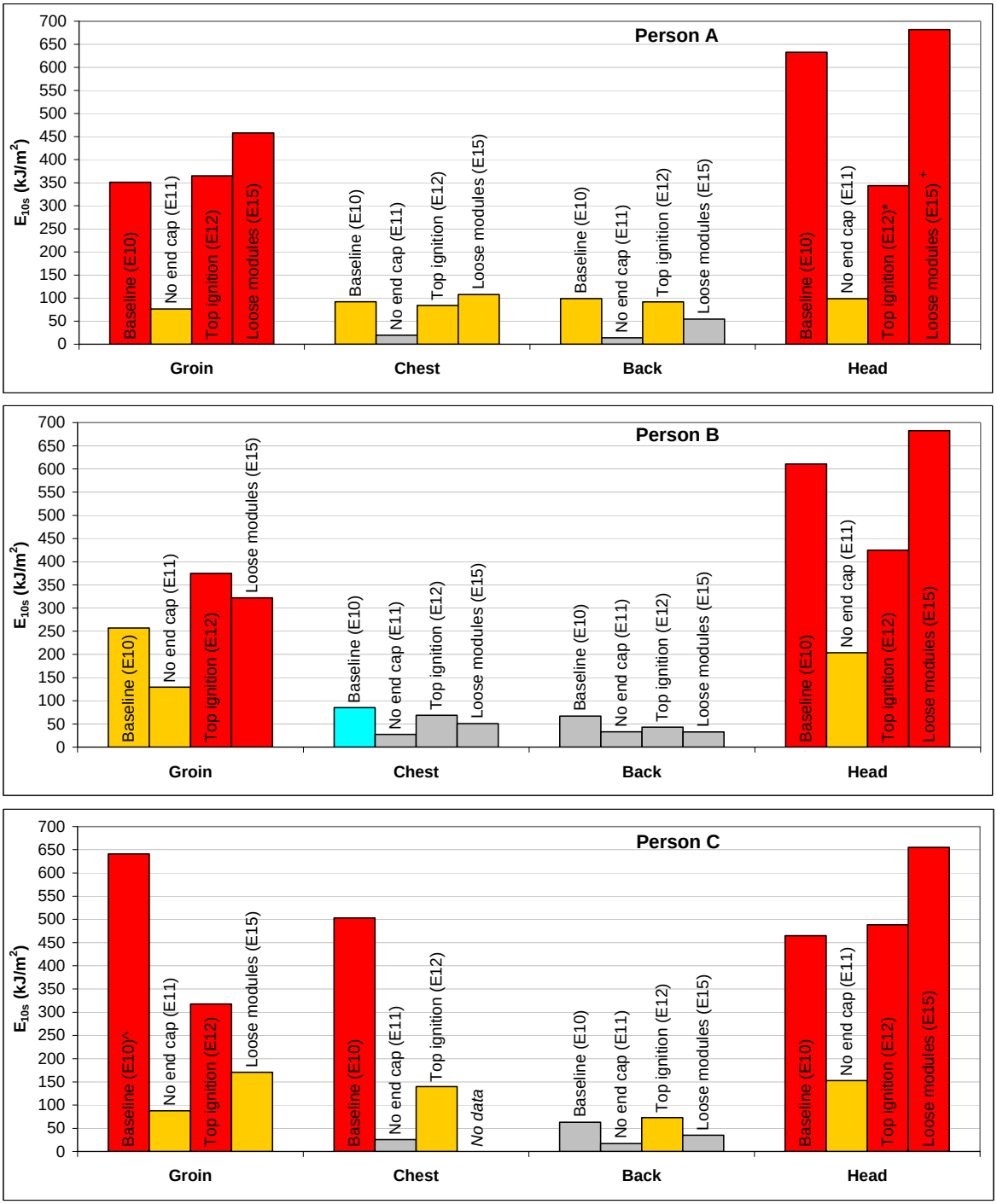

Figure 16: Effect of different module storage and ignition point conditions on 10 s personnel energy absorption for 3xBCM configuration

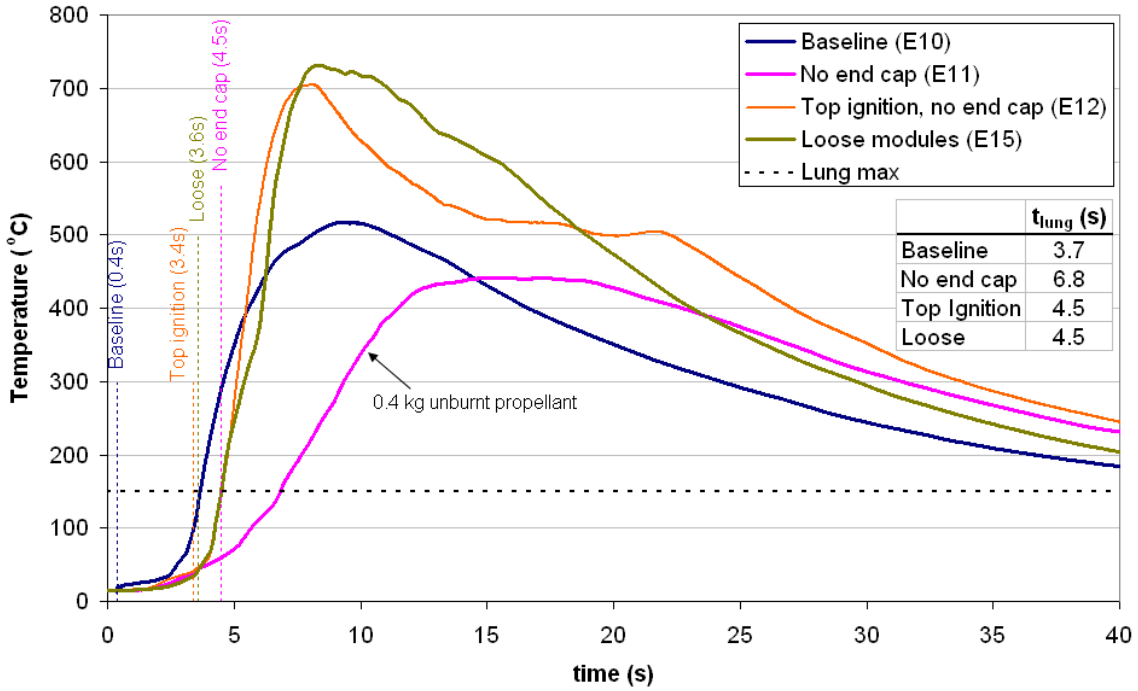

Figure 17: Average crew compartment temperature for the 3xBCM configuration tested under different module storage and ignition point conditions

The slower rate of energy release associated with Experiment 11 produced a more gradual increase in ambient temperature, and the total energy release was also lower for this configuration owing to 0.4 kg of unburnt propellant. Application of an adiabatic, isochoric energy balance over the 19 m^3 volume of the simulated crew compartment, assumed to be at an initial temperature of 15°C, showed that preventing the combustion of 0.4 kg of propellant would suppress the average room temperature by 35°C.

As was the case for the other experiments conducted without the use of the AFESS, the sustained high ambient temperatures for all of the events considered in this section will present a potential sympathetic cook-off risk. Whilst the thermal hazards posed by the 3xBCM configurations are significant, irrespective of storage configuration or ignition location, the less dynamic nature of the experiments conducted without an end-cap may lend them to more effective suppression with an AFESS.

5.2.2 Ejecta

In the absence of a storage tube end-cap, the peak pressures achieved at the base of the storage tube were significantly reduced, see Section 5.2.3. Owing to this reduced confinement condition, propellant and igniter burning was less developed at the time the modules exited the storage tube, and the modules were ejected whole, at lower velocities and without the presence of loose propellant grain ejecta. Hence, reducing tube confinement by removing the storage tube end-cap reduces both the consequences and the likelihood of an ejecta strike on personnel. This is illustrated in Figure 18 that compares ejecta damage to an aluminium witness plate and the chest and groin of Person C for the 3xBCM configuration with and without a storage tube end-cap.

Lower ejection velocities will have the added benefit of reducing the level of propellant fragmentation associated with grain impact on solid surfaces within the crew compartment. This will help maintain the progressive burning nature of the propellant grains, thus reducing the gas generation rate, and energy release in the early stages of the combustion process. In turn, this will afford the crew a longer period of time to escape the crew compartment from a thermal perspective, see Section 5.2.1. Possible detrimental effects associated with a reduction in storage tube end-cap strength are discussed in Section 5.2.3.

For Experiment 11, where the 3xBCM configuration was base ignited in the absence of a storage tube end-cap, the modules exited the tube as a single module train. Hence, the 50% lethality range was based on the combined mass of 3xBCMs. As there were no propellant grains ejected in the early stages of the event, the propelling charge modules represented the only source of potentially hazardous ejecta. However, Figure 19 shows that the module velocity was well below the 50% lethality range and so is unlikely to pose a life-threatening risk to crew.

For Experiment 12, where the modules were initiated from the top, each of the three modules exited the storage tube individually. The highest module velocity was measured for the middle module with a velocity of 5.6 m/s, well below the 50% lethality range of 28-40 m/s. Module velocities were not measured for the loose module configuration (Experiment 15) as, in the absence of the storage tube to contain the generated igniter gases, once the modules began to lift off the tube baseplate there was insufficient force to accelerate them to any velocity of consequence.

Figure 18: Effect of storage tube confinement on ejecta damage. LHS images: 3xBCM with end-cap (Experiment 10). RHS Images: 3xBCM no end-cap (Experiment 11).

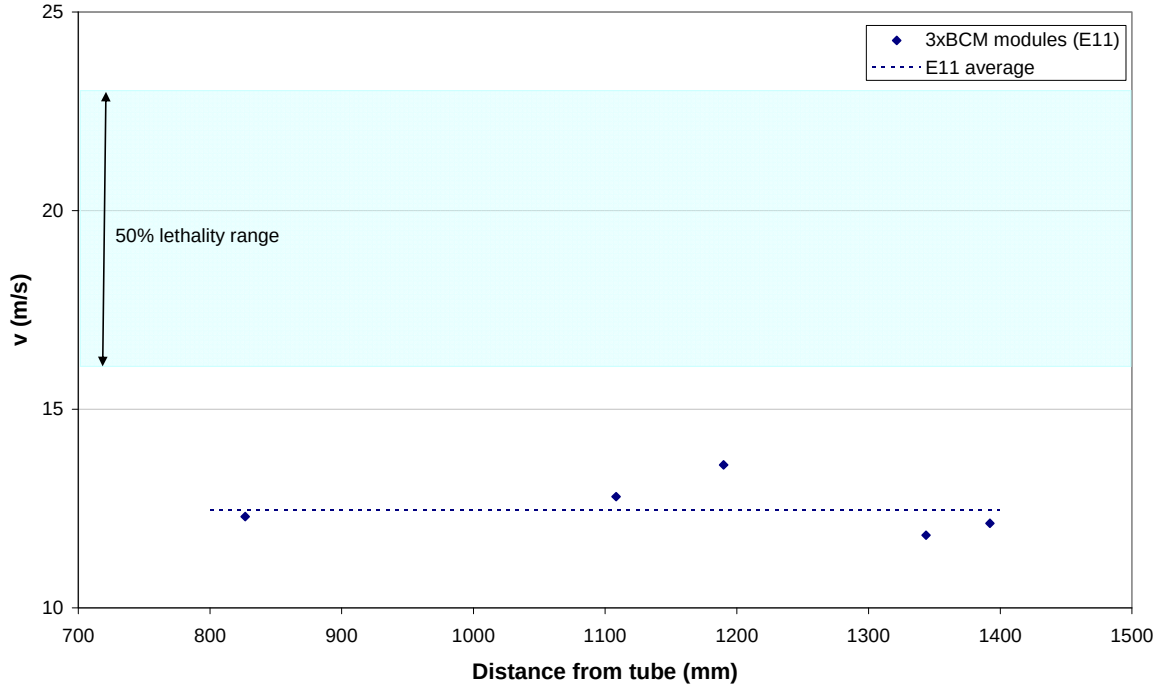

Figure 19: Module velocity as a function of distance from the propelling charge storage tube for the 3xBCM configuration without an end-cap, Experiment 11. 50% lethality range calculated using the blunt force trauma correlation of [11].

5.2.3 Pressure

Figure 20 shows the effect of the storage tube end-cap on the pressure development within the storage tube for the 3xBCM configuration (Experiment 10 and 11). For Experiment 11, given the low magnitude of the observed pressure and for the purposes of visual clarity, the presented pressure-time data was filtered at 50 Hz to remove unwanted signal noise introduced by the grounded pressure sensor. The pressure at the base of the storage tube is a function of the rate of gas generation prior to end-cap failure, and therefore is determined by: match-head initiation; the subsequent commencement of modular charge igniter combustion; the early stages of bulk propellant gasification; and, the level of confinement afforded by the end-cap. The inertia of the module mass also needs to be overcome, but the force required to do this is insignificant when compared with the magnitude of the pressure generated by the other factors.

As discussed in Section 4.1.3, the end-cap was designed to replicate the burst pressure and failure mode of the end-cap used in the represented platform. Reference [1] details the design of the end-cap and quotes a static load at end-cap failure of 750 kPag. A cursory analysis of the experimental storage tube pressure data of Experiment 11 (3xBCM configuration, no end-cap) with that of the 1xTCM configuration[2] with an end-cap (refer to Section 5.4.1 of [1]) was undertaken to verify the aforementioned static failure load.

For the base ignited, no end-cap configuration of Experiment 11 a peak pressure of 1.5 MPag at the base of the storage tube was measured. The failure pressure of the end-cap will be affected by the dynamic nature of the event, with a more dynamic event expected to yield a higher failure pressure. Ignition and combustion development in the storage tube prior to end-cap failure is less dynamic for the 1xTCM baseline configuration than for the 3xBCM configuration and thus, more closely approximates a static load condition. Typical peak base tube pressures of 2.6 MPag were measured for the 1xTCM configuration with a storage tube end-cap in place [1]. For this simple analysis, assuming an additive relationship between the various factors that contribute to the pressure evolution in the tube, this would mean that the presence of the end-cap adds an additional 1.1 MPa to the tube pressure relative to an unconfined tube. The 46% difference between this value and the static design value of 750kPag could be attributed to the dynamic/static deformation relationship of the polycarbonate end-cap coupled with the increased volume occupied by the 1xTCM when compared with the 3xBCM configuration. Hence, in conjunction with the observed 'popping-out' of the end-cap from the storage tube, as predicted from modelling, the above analysis suggests that the end-caps were failing at a representative pressure.

In addition to reducing the possibility of storage tube fragmentation, the reduction in ejecta threats (see Section 5.2.2) and the possibility of enhancing the effectiveness of the AFESS (see Section 5.4), lower storage tube pressures also reduce the peak pressures generated within the crew compartment upon storage tube venting. This reduces the likelihood of intrathoracic over pressure effects or non-life threatening injuries such as auditory damage on personnel.

[2] The 1xTCM configuration is used for comparison with the 3xBCM configuration as it has: the same igniter mass; a similar total volume (6% larger); and, a similar total mass (10% larger).

Figure 21 shows the reduced peak pressures and more gradual ambient pressure rise in the crew compartment afforded by the absence of the storage tube end-cap.

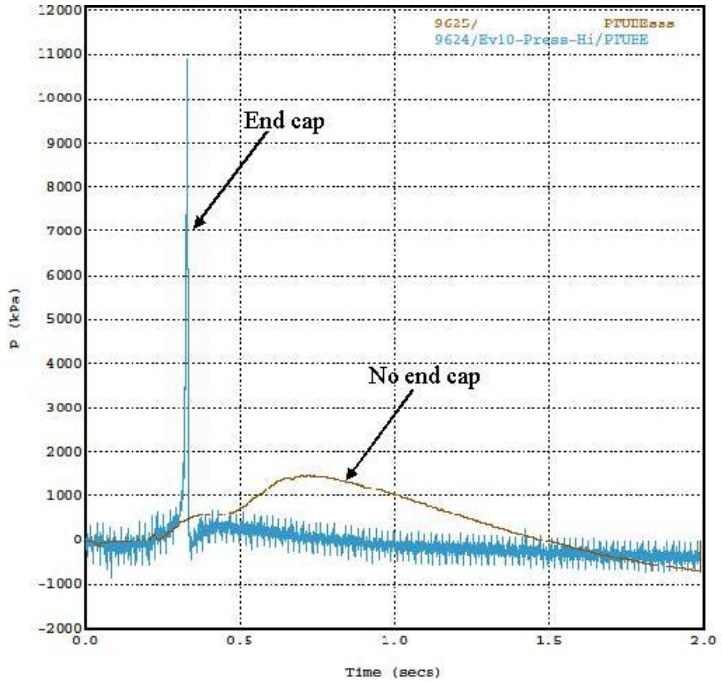

Figure 20: Comparison of storage tube pressure for the 3xBCM configurations tested with and without an end-cap. Data for Experiment 11 filtered at 50 Hz.

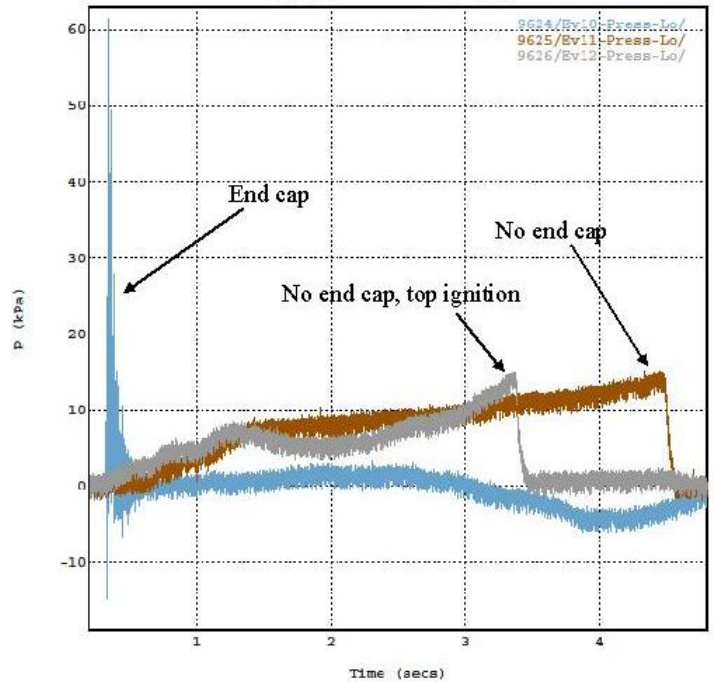

Figure 21: Effect of module storage and ignition point conditions on the ambient crew compartment pressure for a 3xBCM configuration. Pressure measured at the back of Person A.

It should be noted that rapid depressurisation can be an effective means of extinguishing burning propellant. Hence, particularly for the 3xBCM configuration where the tube pressure is highest at the time of end-cap failure, reducing the strength of the end-cap may reduce the level of propellant extinguishment. However, the magnitude of this effect would need to be determined experimentally.

5.3 Clothing

Figure 22 provides a comparison of the energy absorbed at each body location in the 10 s since charge initiation for the non-AFESS experiments conducted over the course of the trial. To permit a direct comparison between energy absorption and body location, in instances where sensors were damaged, it was necessary to calculate the energy absorption over a shorter time duration. This is noted on the figure. Where there is no data provided for a particular body location, the sensor was damaged too early after charge initiation (< 3 s) to permit a meaningful comparison.

It should be noted that the thermal protection afforded by the clothing will vary with time as a result of factors such as: loss of structural integrity owing to thermal damage; clothing ignition after exposure to sustained, high heat flux levels; variation in insulation properties of the fabric as it thermally degrades; and the thermal lag associated with the clothing and any small air gaps between the back face of the fabric and the instrumentation boards. As the applied heat fluxes were transient in nature a rigorous assessment of these factors is not possible, and indeed, is beyond the scope of this study. However, a general statement based upon observations made throughout the trial and from the collected experimental data is that the thermal protection afforded by the clothing decreases with exposure time, and that the Nomex and cotton clothing combination provides a greater level of thermal protection for a longer period of time than Nomex alone.

The data presented for Person A and B in Figure 22 illustrates the thermal protection offered by the Nomex (groin position) and the Nomex and cotton (back and chest positions) relative to unprotected skin (head position). Less consistency in these trends was observed for Person C and is due to the position of Person C relative to the propelling charge storage tube. Being positioned almost directly in-line with the storage tube; the groin of Person C was directly impinged upon by a sustained fireball in many experiments. Further, the chest and groin of Person C was often damaged by ejecta exiting from the storage tube, thus mitigating much of the initial thermal protection afforded by the clothing. Examples of this are shown in Figure 23 that shows photographs of the chest of Person C after Experiments 10 and 14.

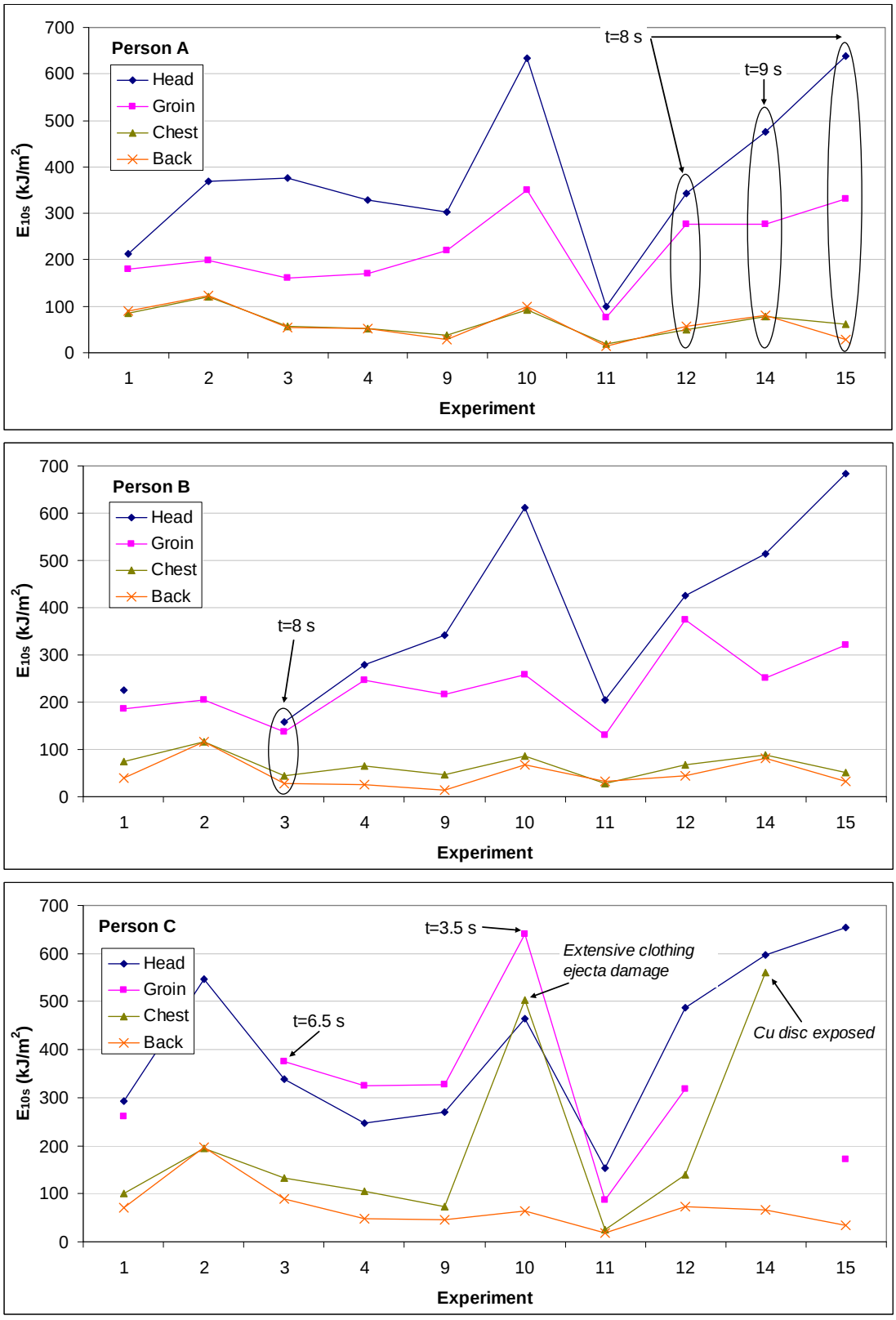

Figure 22: Summary of body location energy absorption for Persons A, B and C for the baseline experiments 10 s after propelling charge initiation

Figure 23: Chest of Person C showing, on the LHS, extensive ejecta damage (Experiment 10) and, on the RHS, exposure of the copper disc (buckled by ejecta impact) owing to ejecta strike during Experiment 14.

To compare the protection afforded by the different clothing combinations (Figure 24), the groin, chest and head of Person B and all body sections of Person A were considered for experiments where the data was not confounded by factors such as burning modules coming to rest beneath an instrumentation board, or extensive fragment damage of clothing. The back of Person B was not considered as it is better protected from radiative heat transfer than the front of Person B. Person C was not considered due to the non-uniformity in incident heat flux across the body locations at this position.

Figure 24 provides a comparison between the average reduction in energy absorption over the first 10 s of the propelling charge event afforded by Nomex and by Nomex coupled with cotton relative to the energy absorbed in the absence of clothing (taken as the energy absorbed by the head). The average reduction in energy absorption for the Nomex, relative to an exposed body part, was 30%. For the Nomex with cotton underlay the average reduction in energy absorption, relative to an exposed body part, was 80%.

An example of typically observed thermal protection afforded by the clothing is shown in Figure 25 for Person A. The heat flux profiles show that the chest and back, covered by Nomex and cotton, is protected from the thermal environment for longer than the groin covered by a single layer of Nomex, which is protected for longer than the exposed head. Whilst affording a level of protection from the thermal environment, once the thermal insult has been removed, if the structural integrity of the clothing remains, then it continues to insulate the skin from the ambient environment, thus delaying the rate of cooling.

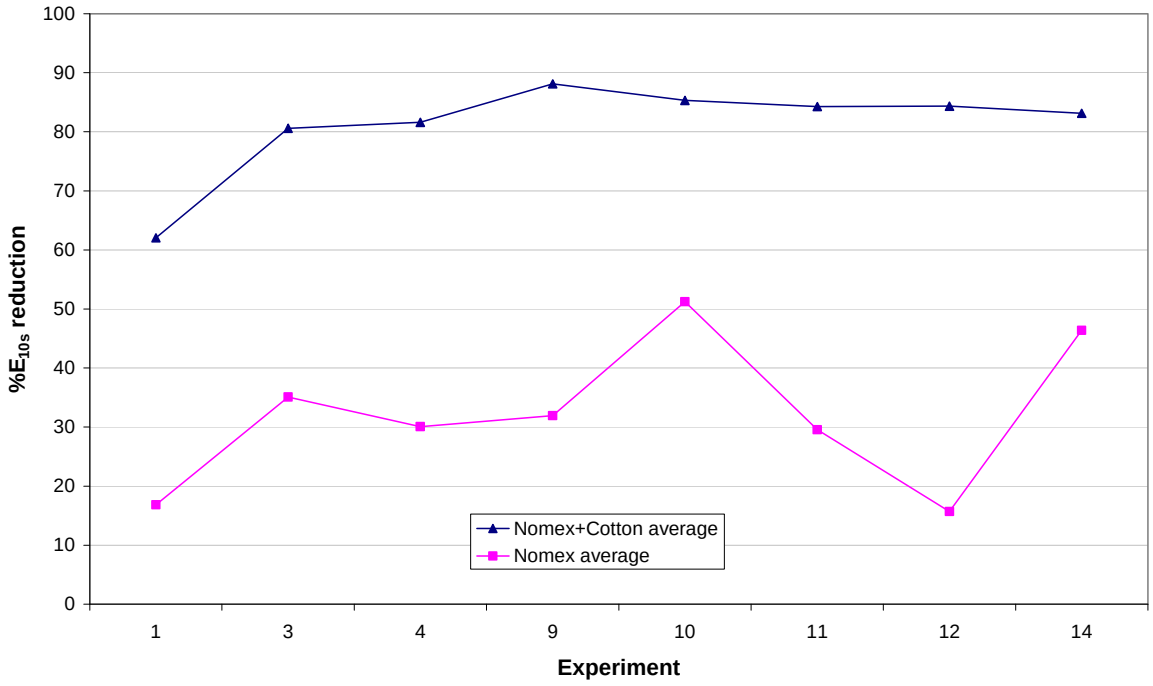

Figure 24: Reduction in skin energy absorption afforded by clothing after 10 s exposure, relative to unprotected skin.

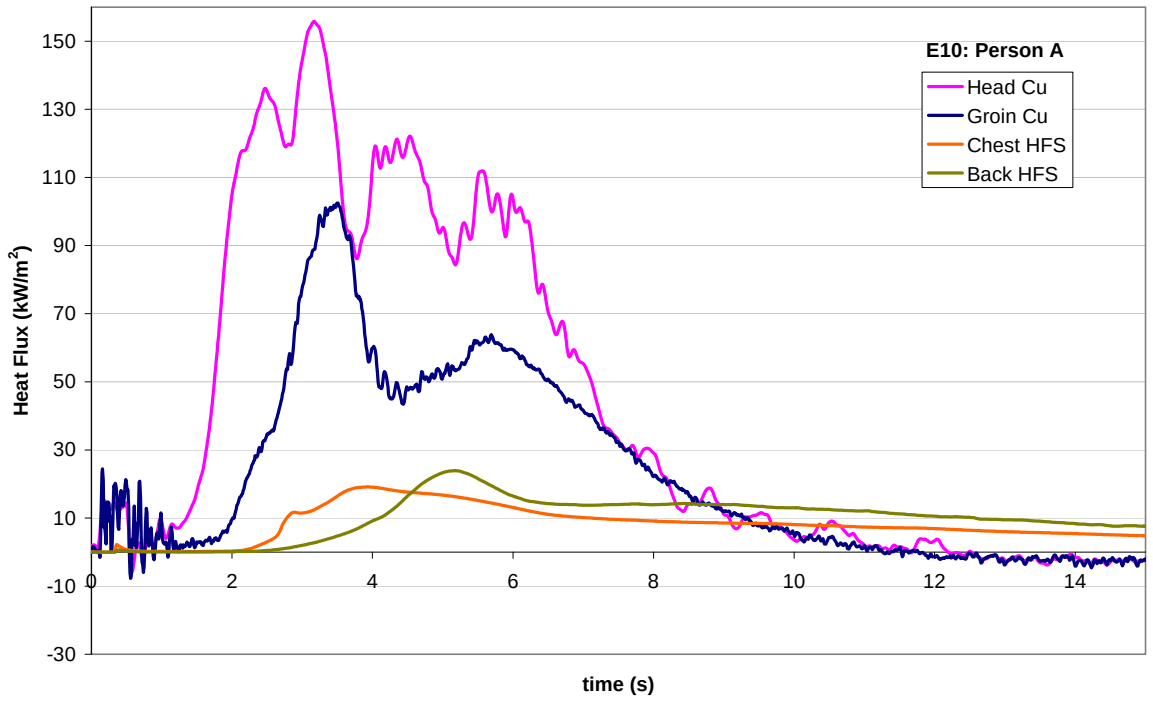

Figure 25: Heat flux profiles demonstrating the effect of clothing on the heat flux absorbed by the skin (Person A, Experiment 10).

5.4 AFESS

5.4.1 Open-Air Tests

Table 11 compares the performance specification for AFESS extinguisher valve action times and suppressant discharge times as required by the US Army Tank-Automotive and Armaments Command (for Class 3 extinguishers filled with Halon 1301, bromo tri fluoromethane, and pressurised to 5.2 MPa with dry nitrogen) [21] with more stringent specifications that have been cited for comparable platforms considered for introduction into service in Australia.

Table 11: Key AFESS extinguisher performance specifications

	MIL SPEC [21]	Australian example
Valve action time (ms)[1]	10	10
Maximum liquid phase discharge time (ms)	270	90

[1]Time from receiving an activation signal (28 V dc step input at 25 ± 8 °C) to commencement of agent release

Results from the open air test firings of the three extinguisher configurations used in the trial are shown in Table 12 and Figure 26 to Figure 28. For scale, in the side-on view the extinguisher nozzle stands 1600 mm off the ground. For the end-on view the distance between the inside of each set of vertical black marks is 500 mm.

Table 12: Open air extinguisher test results

Extinguisher	Fill P (MPa)	Mass before (kg)	Mass after (kg)	Valve action time (ms)	Discharge v (m/s)	Discharge angle[3] (degrees)
Gas	5.2	12.6	7.6	7.5	48	110
Gas, no nozzle	4.8	12.5	7.6	8.5	85	34
Water	6.2	10.4	7.6	8.0	18	100

The valve action times for each of the extinguishers tested satisfies the performance specifications in Table 11. FM200 has a boiling point of 257 K and a vapour pressure of 458kPa at 25 °C [17]. For effective, uniform suppressant dispersion the use of a suppressant with a low boiling point and high vapour pressures is preferred as it reduces the quantity of the suppressant that exits the nozzle as a liquid. Particle image velocimetry studies performed on Class 2 cylinders filled with FM200 showed that only 0.021 – 0.071% (v/v or w/w not reported) FM200 exited the nozzle as a liquid [14]. If it is assumed that the discharge characteristics of the Class 3 cylinders yield liquid phase quantities of the same order of magnitude, it would be expected that the liquid phase discharge times would be very short. Indeed, the performance specification from reference [21] is based upon the use of Halon 1301 as the suppressant agent which has a significantly lower boiling point (215 K) and higher vapour pressure (1620 kPa) than FM200. This would be expected to make the quantity of

[3] The angle as measured at the vertex (i.e. nozzle end) of the discharge 'cone'.

liquid discharged with Halon 1301 smaller than if using FM200. With such a small percentage of the suppressant being discharged as a liquid, the use of a maximum liquid phase discharge time seems largely irrelevant for agents of this type.

From the camera images in Figure 26 through Figure 28, suppressant discharge was still considerable 270 ms after the extinguisher valve had opened for all extinguishers, but in particular for the two gas configurations.

Suppression system effectiveness is enhanced by minimising the time from onset of a fire to complete agent discharge. As would be expected, the absence of a nozzle on the second open-air test (see Figure 27 and Table 12) resulted in a more constrained, higher momentum gas jet than did the gas extinguisher fitted with a nozzle. Such a configuration would be beneficial if the location of a fire was known *a priori* as the suppressant discharge would offer more direct and rapid quenching at the source of the fire. However, in a crew compartment environment where the source of the fire is not known and where the presence of clutter necessitates a wide spreading, uniform suppressant agent discharge, the use of an extinguisher with a nozzle is essential. The extinguisher charged with water had a discharge angle similar to that of the comparable gas extinguisher, but, due to its greater surface tension, density and viscosity had a significantly lower discharge velocity. There was also less symmetry with the water discharge, however, this may be attributed to the use of an extinguisher nozzle optimised for gas rather than liquid dispersion.

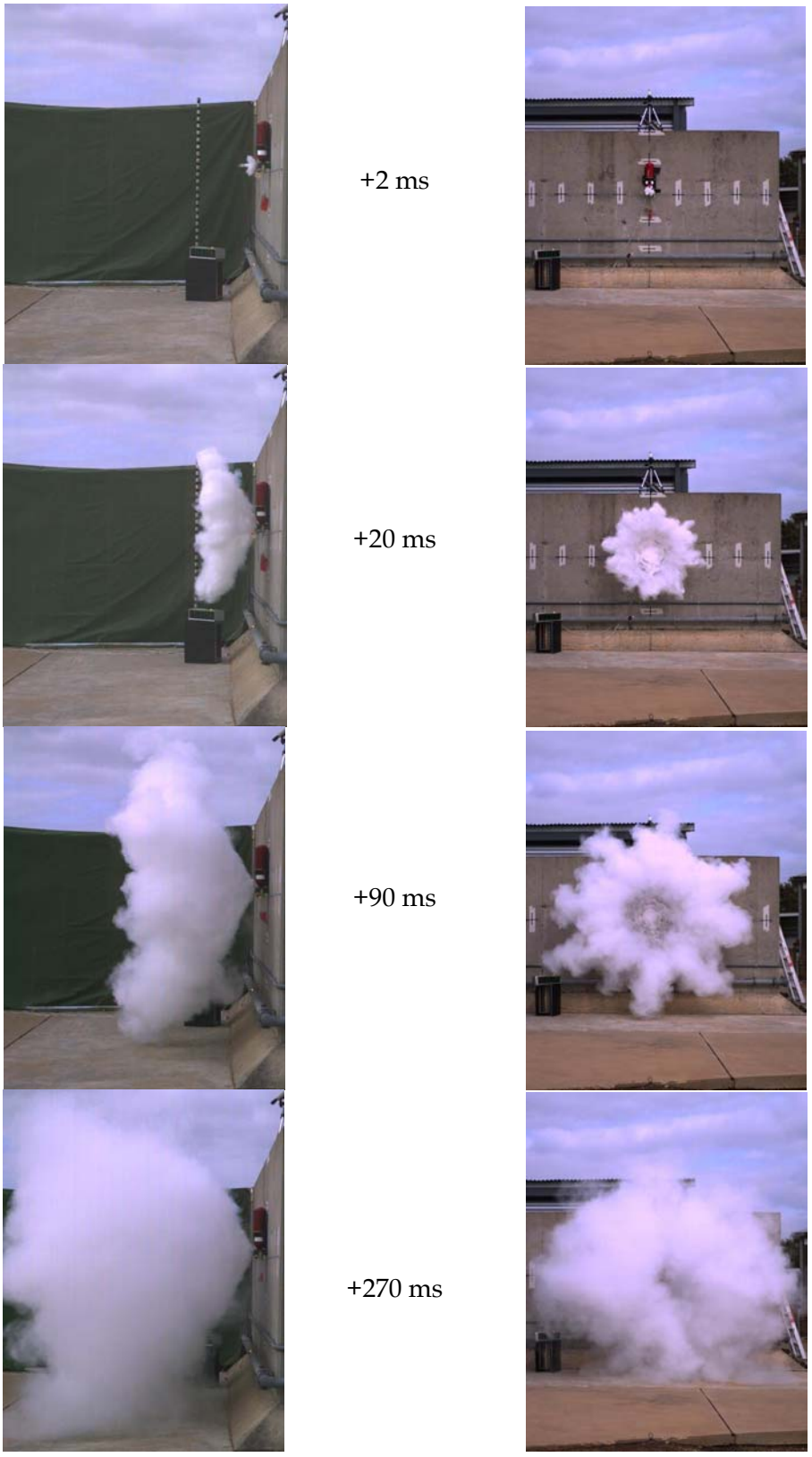

Figure 26: Open air firing of gas extinguisher with nozzle from two viewing angles. Numbers denote time (ms) since agent discharge from the nozzle was first evident.

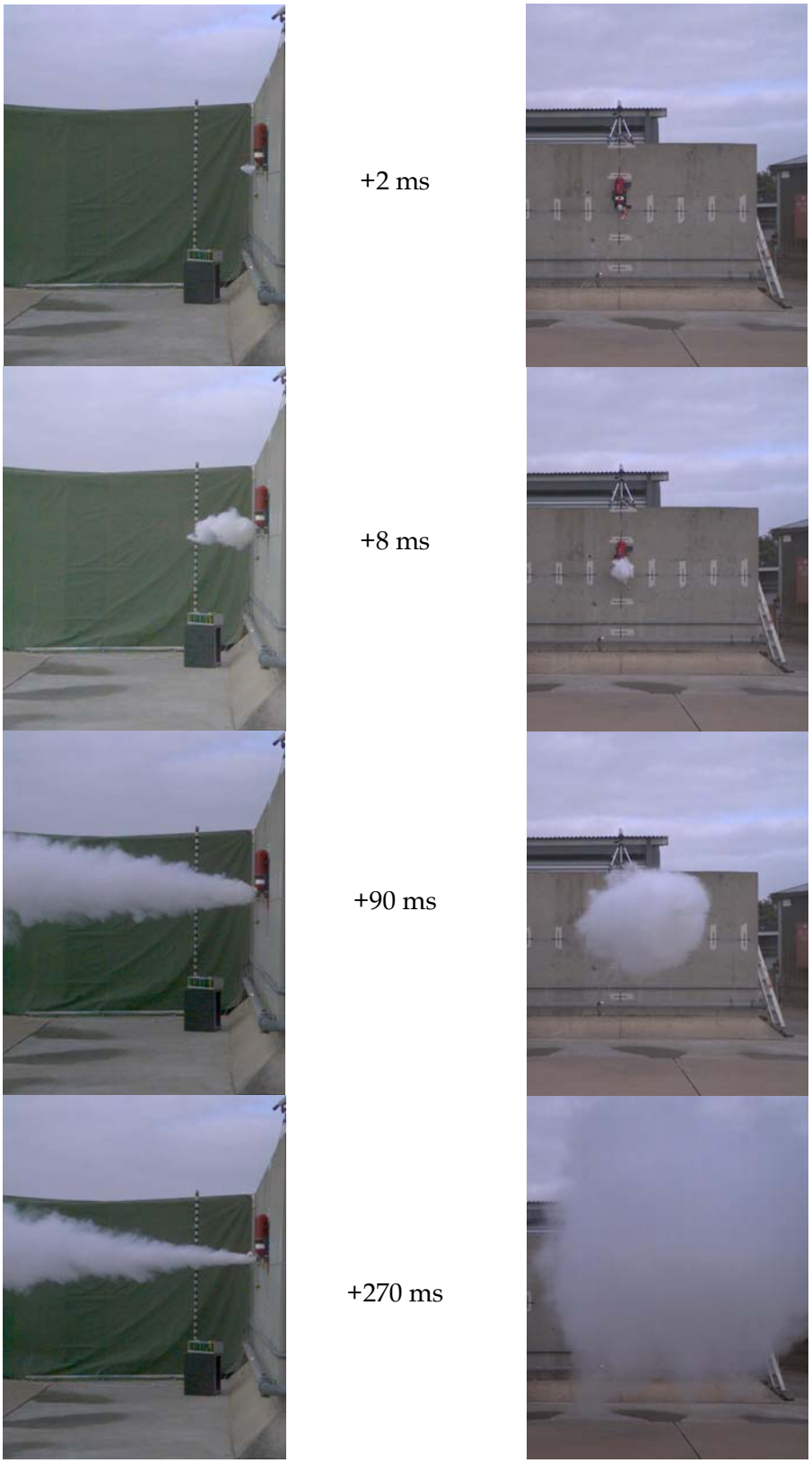

Figure 27: Open air firing of gas extinguisher without nozzle from two viewing angles. Numbers denote time (ms) since agent discharge from the nozzle was first evident.

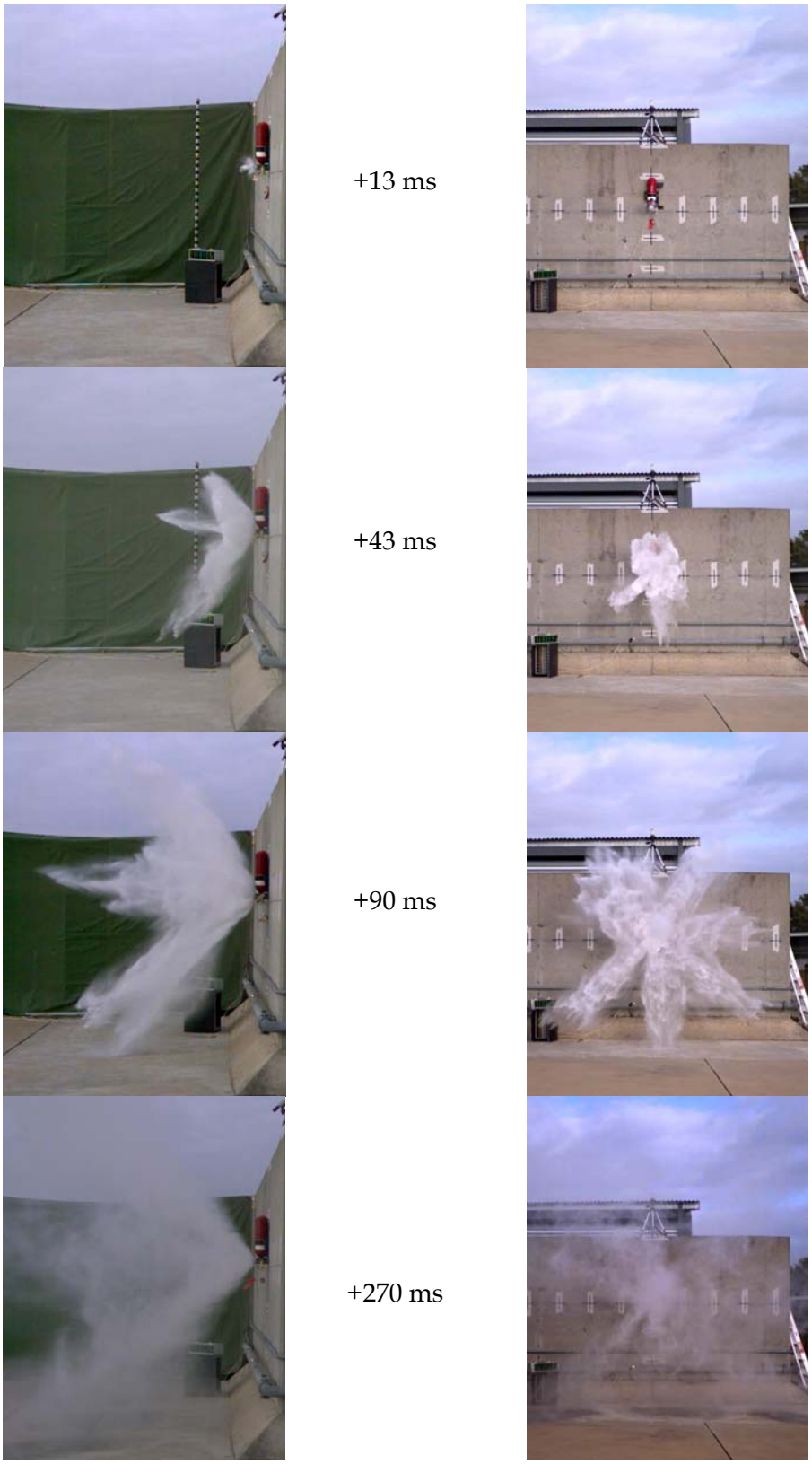

Figure 28: Open air firing of extinguisher charged with water from two viewing angles. Numbers denote time (ms) since agent discharge from the nozzle was first evident.

5.4.2 Effect on Thermal Environment

The effectiveness of the standard AFESS configuration, consisting of four Class 3 gas-filled extinguishers, at reducing crew personnel burn levels through the suppression of propellant combustion and ambient crew compartment temperature reduction is addressed in this section. The effectiveness of the alternative suppression system configuration that employed two additional Class 3 extinguishers, each filled with water, is also addressed. Specific hazards associated with the use of the AFESS are addressed in Section 5.4.3.

Common to all experiments conducted, the AFESS reduces the rate of personnel energy absorption and does so via a number of mechanisms. Upon discharge, the AFESS envelopes the crew in a low temperature discharge; the suppressant absorbs energy from propellant combustion, thereby slowing the rate at which the ambient temperature increases; and the suppression of the ambient temperature delays the rate at which unburnt propellant ejected from the storage tube autoignites. In certain cases, the level of thermal suppression was sufficient to prevent a quantity of propellant igniting, and in these instances, the total amount of energy released is also reduced.

Two identical AFESS experiments were conducted for the 2xBCM configuration and the results are presented in Table 13 and Figure 29 to Figure 31. In the ambient temperature-time plots, the vertical dashed lines correspond to the time when the plywood vent hatch separated from the trials structure. For the first AFESS experiment (Experiment 5), 3.2 kg of unburnt propellant was collected post-test. For the repeat experiment (Experiment 8), 1.9 kg of unburnt propellant was collected. For both AFESS experiments the 10 s energy absorption was greatly reduced relative to the baseline test to the point where only Person C incurred burn damage to the skin. Because of the slower rate of personnel energy absorption owing to the AFESS, there was no difference between the burn damage to the personnel, save for the head of Person C, after a 10 s exposure time in Experiments 5 and 8. However, as the total energy released was higher for Experiment 8, owing to the additional 1.3 kg of consumed propellant, the level of sustained burn damage was notably worse after 30 s exposure; see Table 13(b).

As shown in Figure 30, the reduced propellant consumption in Experiment 5 (AFESS#1) had a pronounced effect on the ambient temperature condition in the crew compartment. The combined effect of lower gas generation and lower temperatures on the internal pressure of the crew compartment kept the pressure below the 13 kPag required to blow off the vent hatch. Retention of the vent hatch would also limit the influx of atmospheric oxygen into the trials structure, thus reducing the energy release associated with secondary combustion of the fuel-rich propellant combustion products. For this suppression event, ambient temperatures were kept below the maximum escape temperature threshold and the thermal environment created by Experiment 5 would not pose a life-threatening risk to crew. Conversely, for the repeat AFESS experiment, Experiment 8 (AFESS#2), Person C would suffer significant burns, incurring 2nd degree burns to the head and groin after 5 s, and the crew would have 6.4 s to exit the crew compartment before the escape threshold temperature was reached. The potential for sympathetic cook-off of other munitions in the crew compartment also exists for Experiment 8.

The ambient temperature-time plots of Figure 30, Figure 34 and Figure 37 use the average of the *T1* and *T2* thermocouples which are positioned at approximately head-height (1.8 m and 2.2 m respectively above the floor), as it is the temperature in the crew compartment at this height which is of interest from a respiratory hazard perspective.

Inspection of the *T3* temperature data (Figure 31, Figure 35 and Figure 38), measured 340 mm off the floor, for the AFESS experiments gave an insight into the means by which the AFESS affected the mass of burnt propellant and also provides supporting evidence for the proposed sequence of events for the propelling charge events. For example, for the 2xBCM configuration, reference [1] describes the sequence of events whereby the upper module is ejected from the storage tube with a portion of unburnt propellant grains falling from its base. This upper module then strikes a solid surface and further scatters unburnt grains throughout the crew compartment. The lower module remains in the storage tube. Ignited by the match-head, the bulk of this lower module and its propellant burns in the storage tube and escalates into a high intensity fire that emanates from the storage tube. During the early stages of this process, high storage tube pressures eject both unburnt and burning propellant and other modular charge components from the lower module retained in the tube. Burning firebrands fall to the ground causing localised spot fires which then spread to nearby propellant grains scattered around the crew compartment floor, the ambient temperature increases above the propellant ignition temperature and a mass fire develops.

If the temperature near the ground, where the unburnt propellant is dispersed post-ignition, can be suppressed below the propellant ignition temperature (approximately 165 °C), then a portion or all of the unburnt propellant ejected from the storage tube can be prevented from igniting. This reduces the total energy released and suppresses the ambient crew compartment temperature. This is demonstrated in Figure 31 where, for the 2xBCM configuration of Experiment 5, the FM200 suppressant, which is denser than air, accumulates at ground level and keeps the temperature well below the propellant ignition temperature. This prevented the ignition of a propellant mass roughly equivalent to the mass of the upper module plus a portion of unburnt propellant grains from the bottom module that were ejected from the tube shortly after end-cap failure. For Experiment 8, a smaller portion of unburnt propellant was collected post-test as the temperature in the vicinity of the floor exceeded the propellant ignition temperature for a 12-13 s period at the position at which *T3* was measured.

Table 13: Burn charts for 2xBCM configuration showing effect of the AFESS at (a) 10 s personnel exposure, (b) 30 s personnel exposure

(a) 10 s exposure		**Person A**				**Person B**				**Person C**			
2xBCM	Experiment	Groin	Chest	Back	Head	Groin	Chest	Back	Head	Groin	Chest	Back	Head
Baseline	4	8	-	-	4,19	6	-	-	6,42	4,19	8	-	5
AFESS#1	5	-	-	-	-	-	-	-	-	7	-	-	-
AFESS#2	8	-	-	-	-	-	-	-	-	5	-	-	5

(b) 30 s exposure		**Person A**				**Person B**				**Person C**			
2xBCM	Experiment	Groin	Chest	Back	Head	Groin	Chest	Back	Head	Groin	Chest	Back	Head
Baseline	4	8,32	14	14	4,17	6,23	12	-	6,20	4,16	8	18	5,21
AFESS#1	5	-	-	-	-	-	-	-	-	7	-	-	-
AFESS#2	8	-	-	25[e]	24	-	-	-	19	5	22	-	5

a,b	3rd degree burn, a=time to 2nd degree burn (s), b=time to 3rd degree burn (s)
a	2nd degree burn, a=time to 2nd degree burn (s)
a	1st degree burn, a=time to first degree burn (s)
-	No burn sustained

[e]Burning grain on sensor

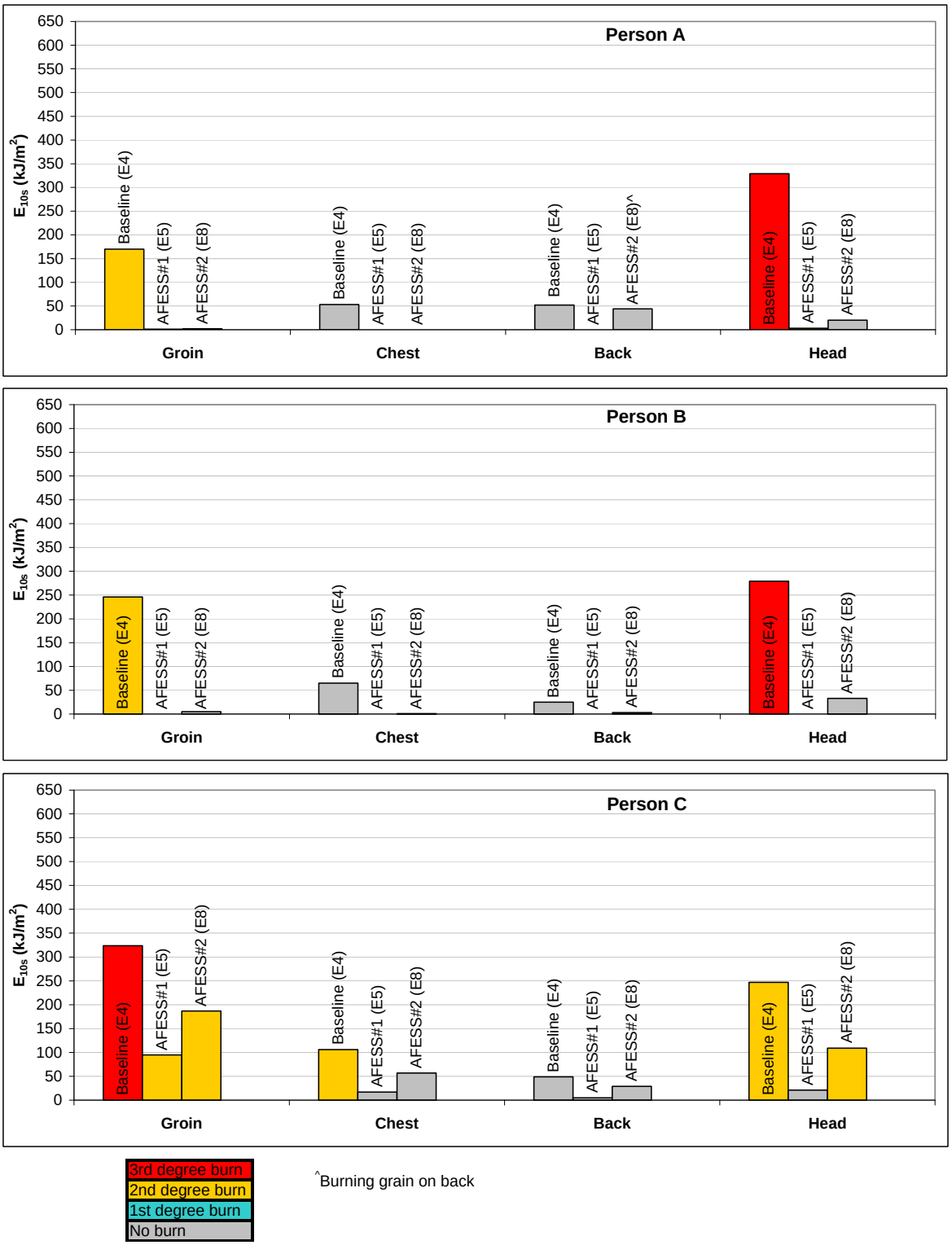

Figure 29: Effect of the AFESS on energy absorbed by the skin after 10 s exposure for 2xBCM configuration.

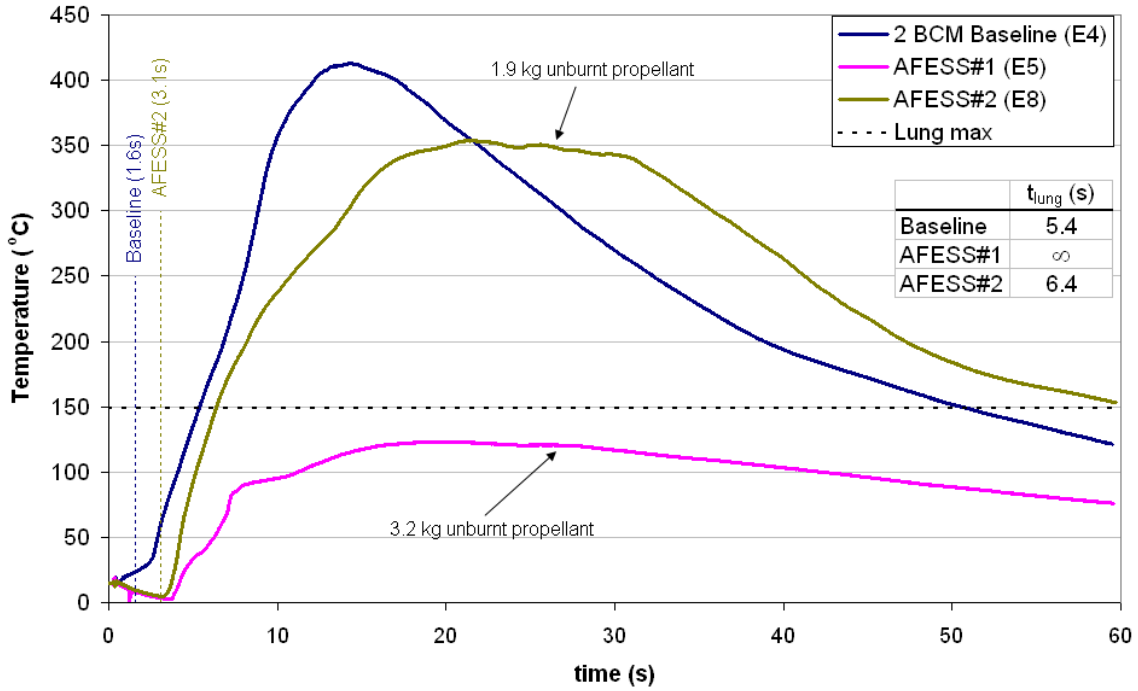

Figure 30: Effect and repeatability of the AFESS on the ambient crew compartment temperature. 2xBCM configuration. Temperature data is the average of thermocouples T1 and T2.

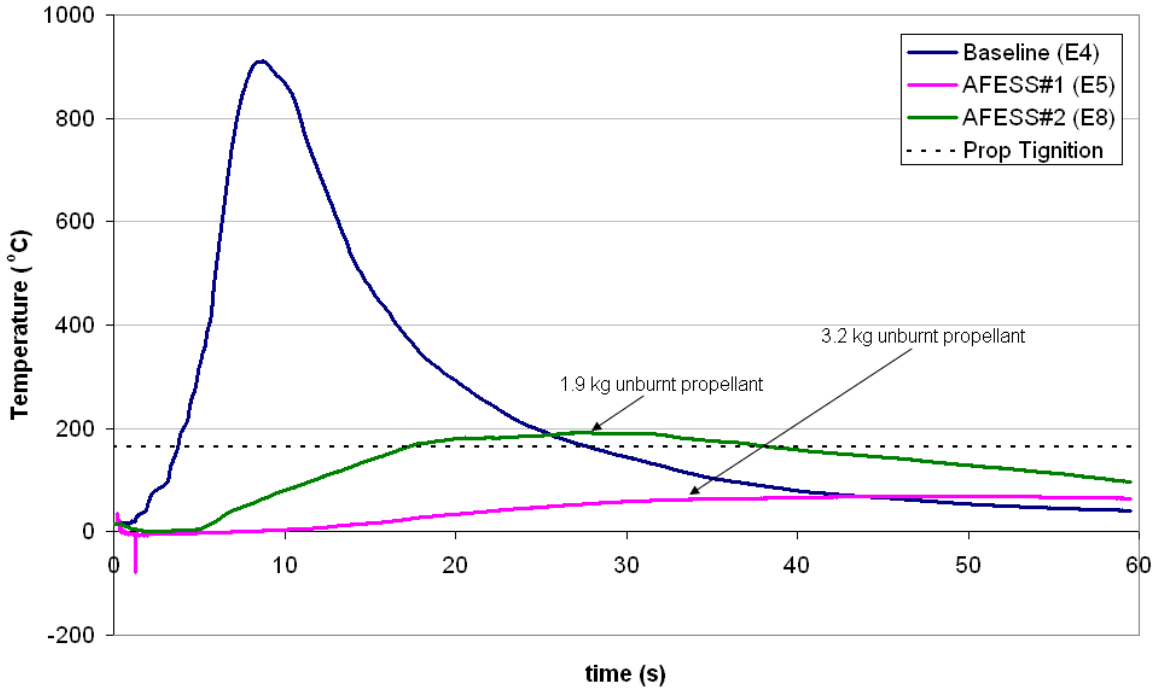

Figure 31: Effect of the AFESS on crew compartment temperature close to ground level (T3) for the 2xBCM configuration.

From the data presented in Table 14, the difference in AFESS effectiveness for Experiments 5 and 8 cannot be attributed to the AFESS response time, as all else being equal, a shorter AFESS response time should result in more effective suppression. Comparison between the *average quickness*[4] for Experiment 5 and 8 indicated enhanced ignition development in the storage tube for the modules in Experiment 8 prior to end-cap failure and this would be expected to reduce the effectiveness of the AFESS. Another contributing factor to the noted difference in AFESS effectiveness may be attributed to spatial effects. It is widely reported in the literature (see for example [17,22,23]) that the suppressant delivery method and nozzle orientation has a large effect on suppression effectiveness. For effective suppression the suppressant agent needs to be discharged to the source of the fire as rapidly and as directly as possible. As there was no control over the exit of the modules from the storage tube, or the subsequent distribution of the propellant grains throughout the crew compartment, these variables could have contributed to the noted difference in suppression effectiveness. Owing to the obscuration of the camera footage upon suppression agent discharge, it was not possible to confirm any spatial variance.

Figure 32 shows screenshots from Experiment 5, captured from viewing angle D, that show the initial propelling charge ignition event, followed by suppressant discharge. Where obscuration associated with propelling charge debris did not preclude an observation of the initial AFESS discharge, the time from storage tube end-cap failure to the first sign of AFESS discharge was made. These results are summarised in Table 14.

Table 14: AFESS response time for selected experiments

Configuration	Experiment	$\Delta t_{\text{end-cap fail-AFESS discharge}}$ (ms)	$P_{max}{}^{*}$ (MPa)	*Avg Quickness* (MPa/s)
2xBCM	5	109	2.9	234
2xBCM	8	92	2.8	283
3xBCM	7	9	15.8	3343

*Maximum storage tube pressure

The disparity between the response time for Experiment 7 compared with Experiments 5 and 8 is most likely due to the time at which an 'event' is detected by the optical detector. Whilst there is an initial flash upon end-cap separation from the tube, this may not set off the optical detector in all instances, as in the case of Experiments 5 and 8. The 9 ms discharge time for Experiment 7 suggests that the initial flash occurring at the time of end-cap failure was detected by the optical detectors, thus resulting in a substantially reduced response time which matches closely with the valve action times of the cylinders as determined from open-air testing, see Section 5.4.1.

[4] Average rate of change of storage tube pressure at 40, 60 and 80% of the maximum measured storage tube pressure.

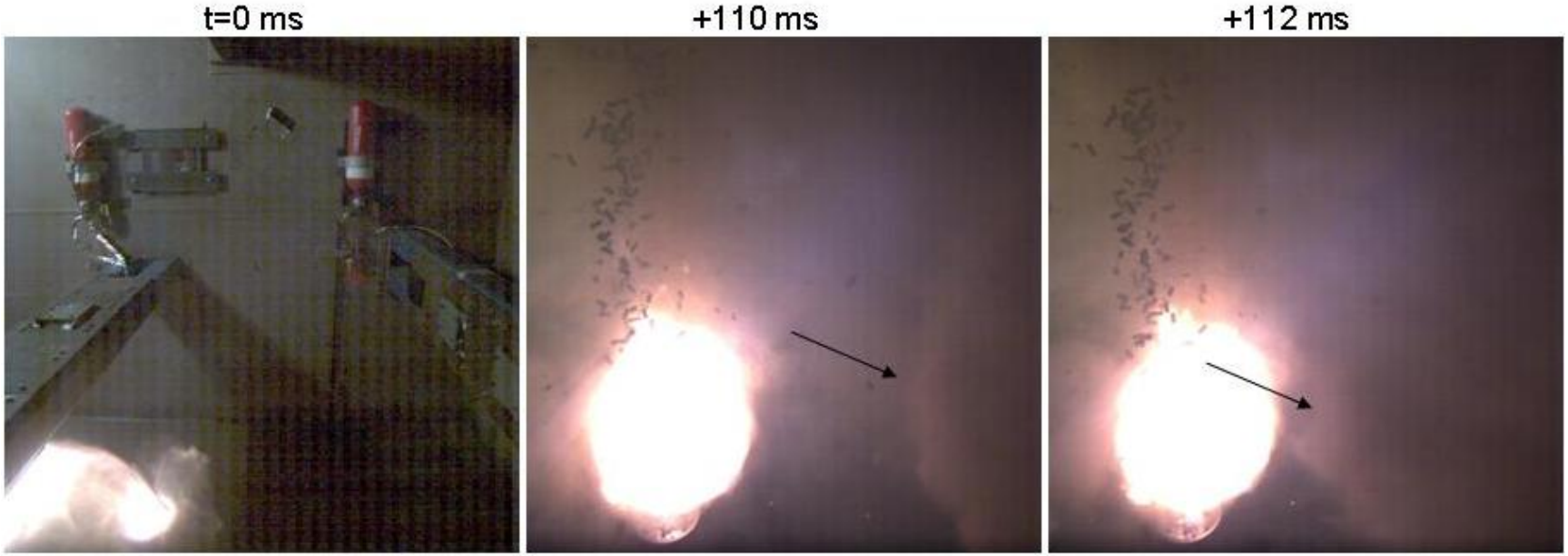

Figure 32: Camera images of Experiment 5 showing end-cap failure, subsequent propellant ejection and then suppressant plume from AFESS discharge (leading front of plume shown with arrows)

Table 15 and Figure 33 to Figure 35 illustrate the benefits afforded by the AFESS on the thermal environment resulting from a 1xTCM event. The standard AFESS (Experiment 6) reduced the rate of personnel energy absorption, but significant burns were still sustained by Person C after 10 s exposure. The initial suppression in the ambient temperature afforded the crew an additional 3 s to exit the crew compartment before the maximum escape temperature was reached. If the propelling charge event does not impair the mobility of the crew personnel, and if the pressure environment does not damage the escape hatches or rear door, the 7.6 s escape time may be adequate time to exit the crew compartment for crew who have not suffered disorientation or loss of cognition.

The incorporation of two water cylinders, containing a combined mass of 6.4 kg of water and pressurised to 6.5 MPag with nitrogen, in addition to the four gas cylinders (Experiment 13), had a marked effect on the thermal environment. 5.8 kg of propellant and combustible case material was collected after the experiment and peak average temperatures in the crew compartment were limited to 70 °C. This 5.8 kg corresponds to the mass of a single TCM less approximately 2 kg of propellant that falls out the base of the module and is retained in the storage tube as the TCM exits the storage tube. This is supported by Figure 35 where *T3* barely exceeds ambient. Thus, any unburnt propellant distributed throughout the crew compartment does not ignite. Inspection of TCM propellant grains post-test also showed that some of the distributed grains that had commenced burning were subsequently extinguished via water cooling of the burning surface (see Figure 42(b) of [1]). Aside from 2nd degree burns to the groin of Person C, resulting from direct flame impingement from the flamethrower effect created in the charge storage tube, no other burn damage to the skin was predicted from the measured data.

Four gas cylinder nozzles were available for the trial. As the modified AFESS setup had six cylinders it was necessary to operate two cylinders without nozzles. In the absence of an extinguisher nozzle, it was assumed that the water discharge would be more affected than the gas discharge. Hence, Experiment 13 was conducted with nozzles on both water cylinders and on two of the four gas cylinders. Due to the more constrained, higher momentum gas discharge associated with the gas cylinder with no nozzle relative to the gas-with-nozzle configuration (see Table 12, Figure 26 and Figure 27), it is not possible to resolve to what level the benefits observed for Experiment 13 were due to: the more directed gas discharge; the incorporation of the water; or a combination of the two.

The rapid failure of the vent hatch in Experiment 13, see Figure 34, can be attributed to the pressure generated by the AFESS cylinder discharge. Complete discharge of the AFESS, with an assumed discharge temperature of 215 K, into a 19 m^3 volume at an initial temperature of 288 K generates a pressure inside the crew compartment of approximately 13 kPag. This is equivalent to the pressure required to blow off the vent hatch.

Table 15: Burn charts for 1xTCM configuration showing effect of the AFESS at (a) 10 s personnel exposure, (b) 30 s personnel exposure

(a) 10 s exposure		**Person A**				**Person B**				**Person C**			
1xTCM	Experiment	Groin	Chest	Back	Head	Groin	Chest	Back	Head	Groin	Chest	Back	Head
Baseline	3	7	-	-	6,16	7	10	-	6[P]	4,<15[°]	8	10	5,19
AFESS	6	-	-	-	9	10	-	-	9	4,14	10	-	7
With water	13	-	-	-	-	-	-	-	-	9	-	-	-

(b) 30 s exposure		**Person A**				**Person B**				**Person C**			
1xTCM	Experiment	Groin	Chest	Back	Head	Groin	Chest	Back	Head	Groin	Chest	Back	Head
Baseline	3	7,25	12	12	6,15	7,22	10	13	6[P]	4,<15[°]	8,29	10	5,16
AFESS	6	12,52	19	21	9,21	10,24	14	18	9,22	4,14	11,33	18	7,22
With water	13	-	-	-	-	-	-	-	-	9	-	-	-

a,b	3rd degree burn, a=time to 2nd degree burn (s), b=time to 3rd degree burn (s)
a	2nd degree burn, a=time to 2nd degree burn (s)
a	1st degree burn, a=time to first degree burn (s)
-	No burn sustained

[°]Cu disc failed at 5.7s at 185°C

[P]HFS delaminated at 8.0 s

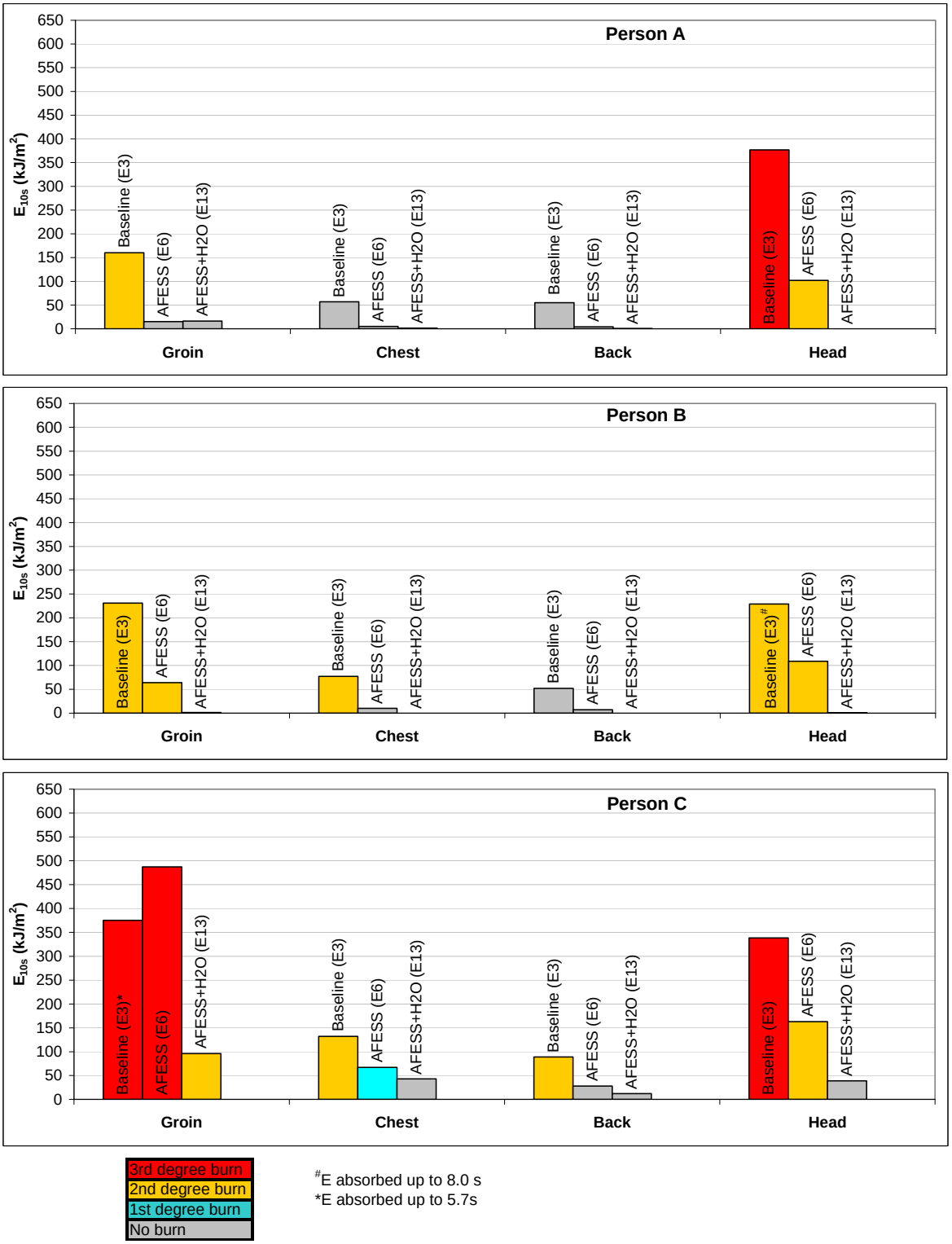

Figure 33: Effect of the AFESS on energy absorbed by the skin after 10 s exposure for 1xTCM configuration.

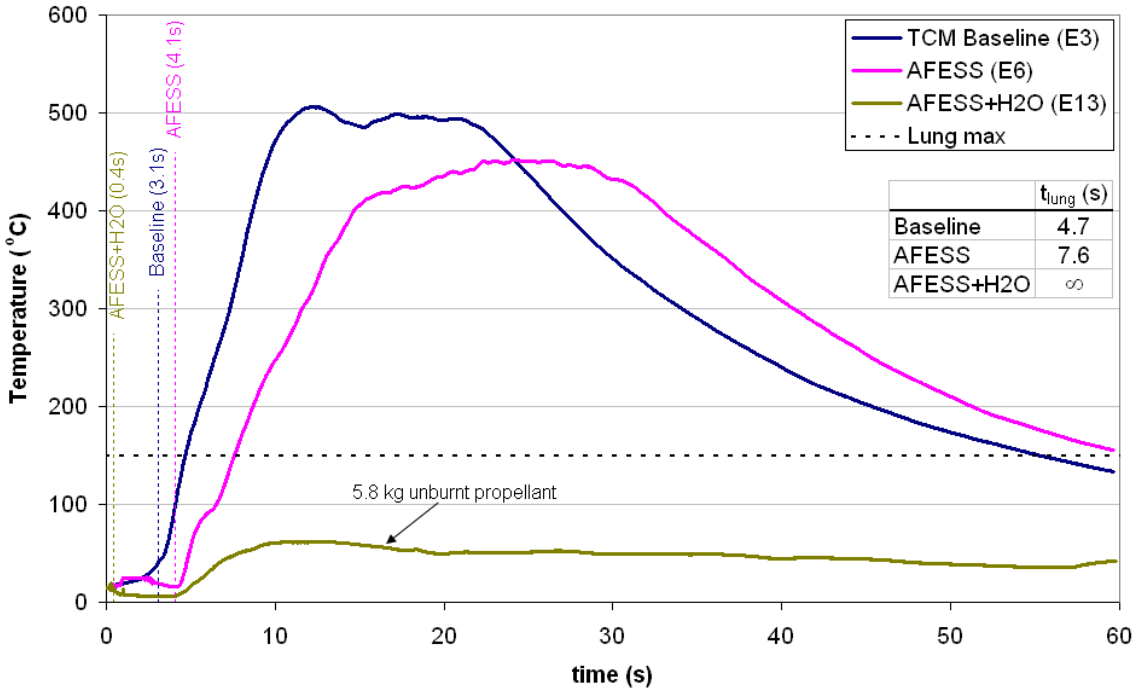

Figure 34: Effect of the AFESS on the ambient crew compartment temperature at head height. 1xTCM configuration. Temperature data is the average of thermocouples T1 and T2.

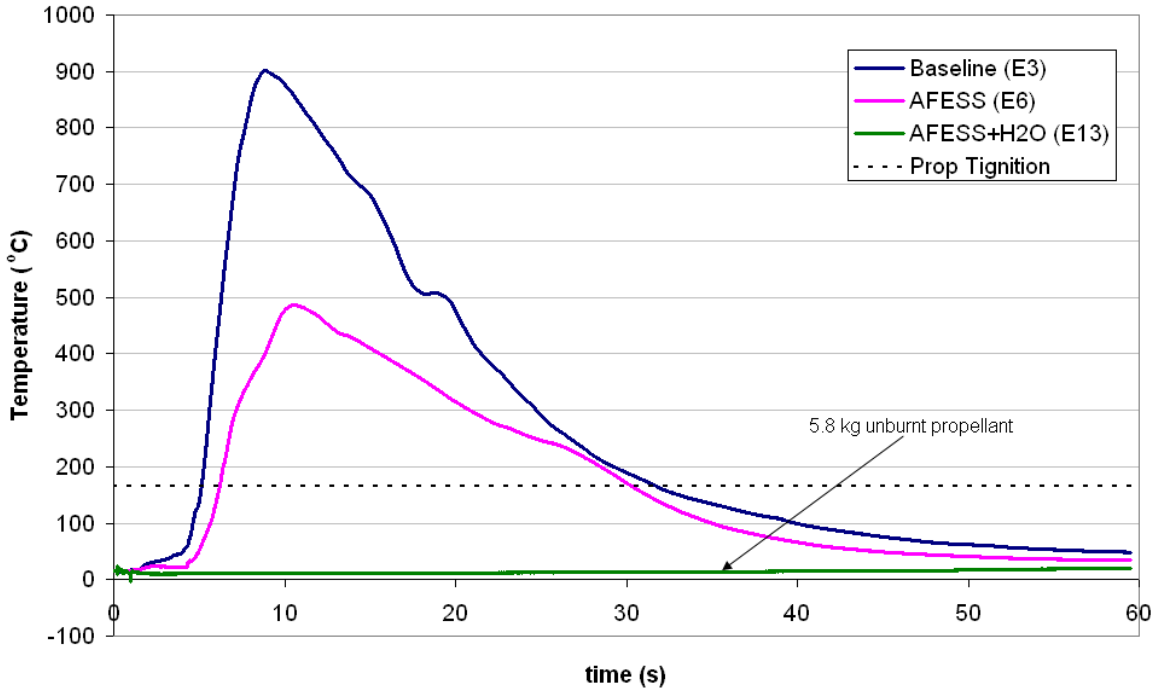

Figure 35: Effect of the AFESS on the ambient crew compartment temperature near ground level (T3). 1xTCM configuration.

Similarly to the other module configurations tested, the AFESS reduced the rate of personnel energy absorption in the 3xBCM configuration (see Figure 36). However, the difference was not as pronounced as for the less dynamic 1xTCM and 2xBCM events. Whilst the AFESS reduced the 10 s skin burn level for Person A and B, as shown in Table 16 and Figure 36, it did not increase the time before the threshold escape temperature was reached (see Figure 37).

All propellant was burnt in both the AFESS and baseline testing of the 3xBCM configuration, thus the total energy released for both experiments was the same. However, for the AFESS case (Experiment 7), the propelling charge combustion event lasted for 18 s. This compares with an event time of 9 s for the baseline case of Experiment 10. The energy release after 10 s for Experiment 7, coupled with the thermal energy absorbed by the AFESS, accounts for the difference in temperature-time profiles between the two experiments in Figure 37 and Figure 38.

For the 3xBCM configuration, the likelihood of fatality due to thermal effects remains high for all personnel irrespective of whether the AFESS is used or not. The sustained, elevated temperatures in the crew compartment also represent the potential for the sympathetic cook-off of other on-board munitions.

Table 16: Burn charts for 3xBCM configuration showing effect of the AFESS at (a) 10 s personnel exposure, (b) 30 s personnel exposure

(a) 10 s exposure		**Person A**				**Person B**				**Person C**			
3xBCM	Experiment	Groin	Chest	Back	Head	Groin	Chest	Back	Head	Groin	Chest	Back	Head
Baseline	10	3,16	9	8	2,10	4	9	-	2,10	1,<7[n]	3,10	-	3,12
AFESS	7	5	-	-	1	8	-	-	2	1,<12[p]	2,12	-	No data[b]

(b) 30 s exposure		**Person A**				**Person B**				**Person C**			
3xBCM	Experiment	Groin	Chest	Back	Head	Groin	Chest	Back	Head	Groin	Chest	Back	Head
Baseline	10	3,16	9	8	2,10	4,28	11	18	2,10	1,<7[n]	3,10	14	3,12
AFESS	7	5,29	16	16	1,22	8	21	-	2,22	1,<12[p]	2,12	20	No data[b]

a,b	3rd degree burn, a=time to 2nd degree burn (s), b=time to 3rd degree burn (s)
a	2nd degree burn, a=time to 2nd degree burn (s)
a	1st degree burn, a=time to first degree burn (s)
-	No burn sustained

[b]Fragment strike

[n]Cu disc failed at 3.5s at 150°C

[p]Cu disc failed at 1.8s

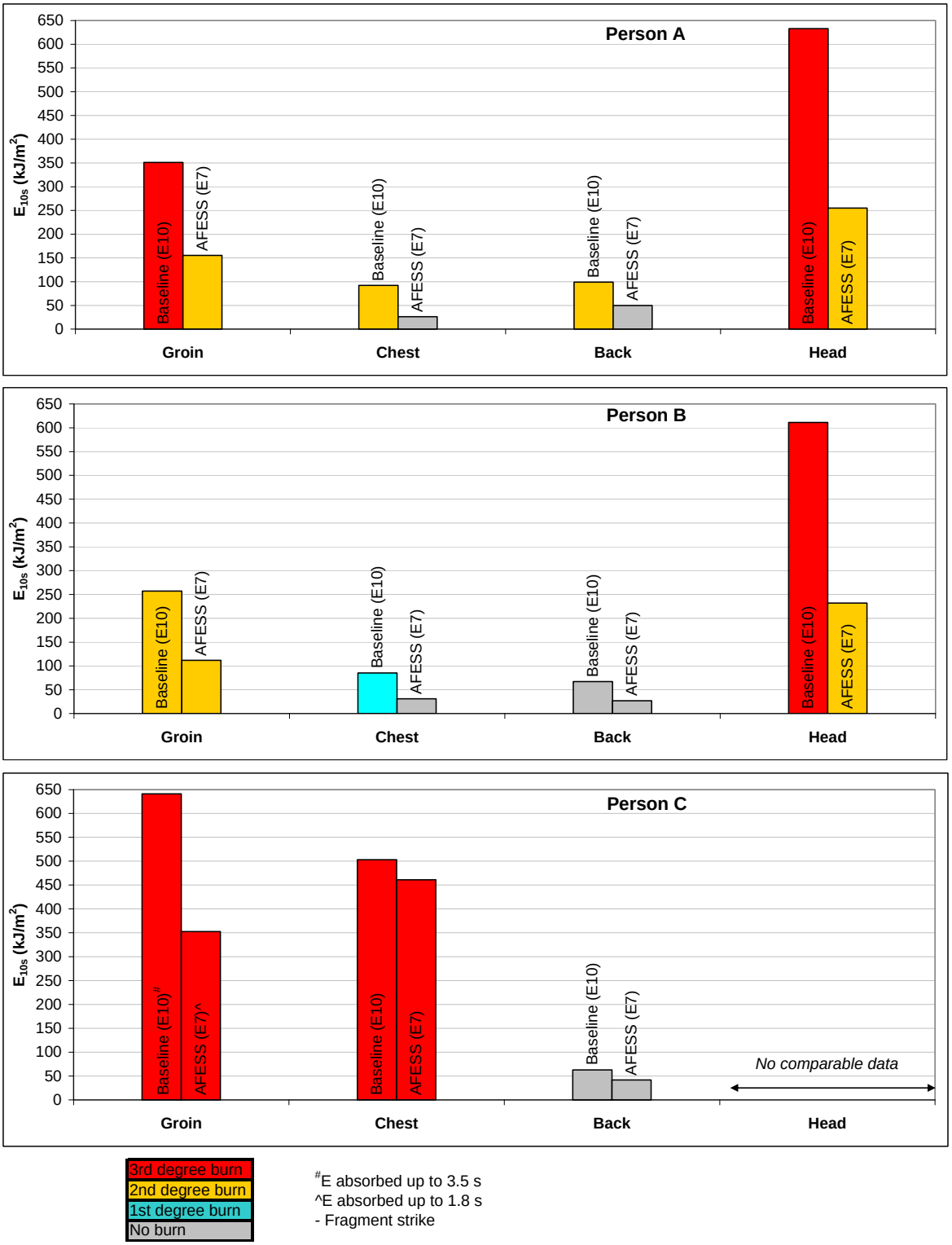

Figure 36: Effect of the AFESS on energy absorbed by the skin after 10 s exposure for 3xBCM configuration.

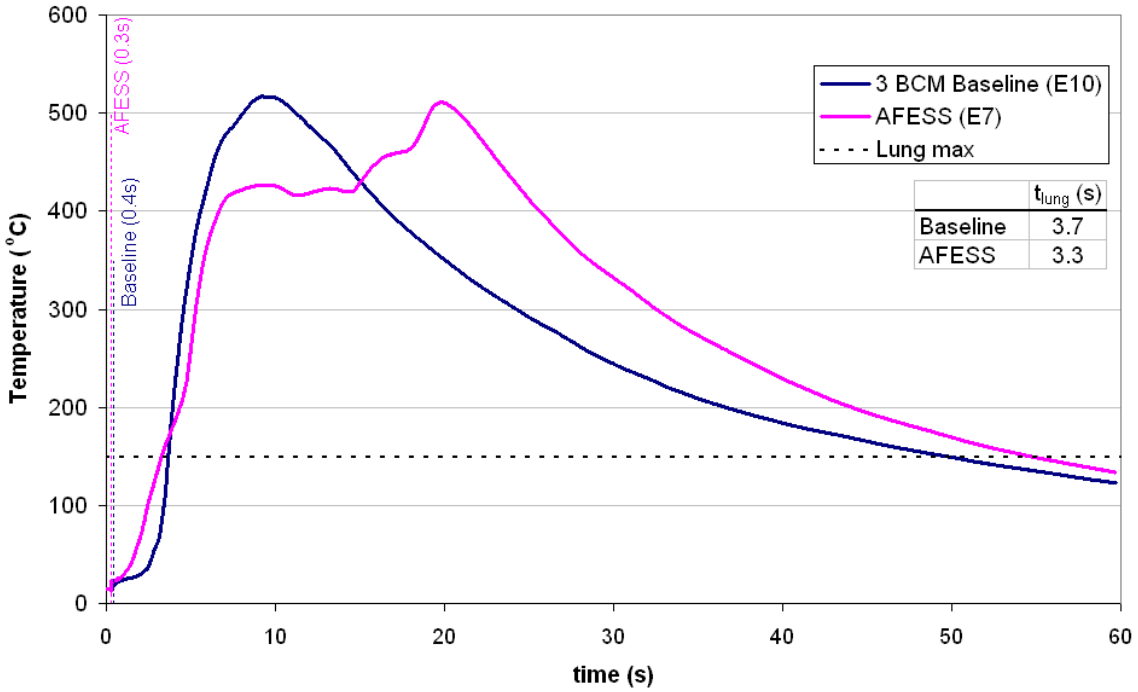

Figure 37: Effect of AFESS system on the ambient crew compartment temperature at head height. 3xBCM configuration. Temperature data is the average of thermocouples T1 and T2.

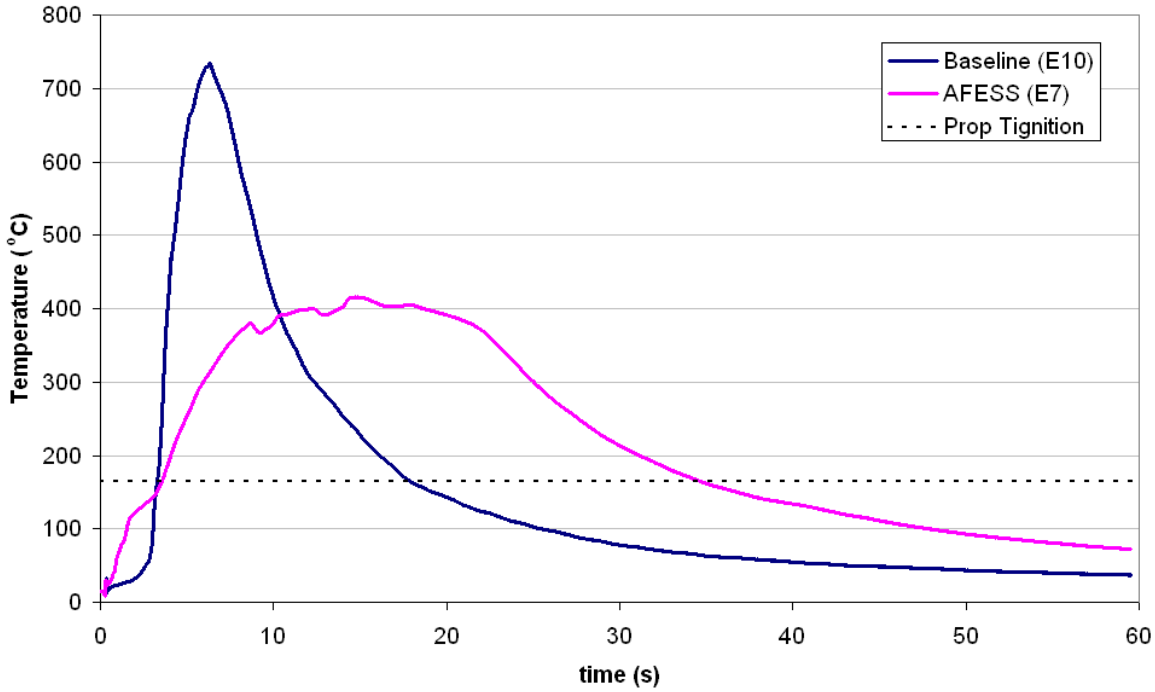

Figure 38: Effect of the AFESS on the ambient crew compartment temperature near ground level (T3). 3xBCM configuration.

5.4.3 AFESS-Specific Hazards

The incorporation of BCS in the extinguishers, and also the use of water, will likely have a detrimental effect on the electrical systems within the crew compartment should the AFESS be discharged. More serious from a crew injury perspective is the possibility of steam production in the event of discharge of a water-containing AFESS into a high temperature environment. Water has a significantly higher heat capacity than the gases that would be present in the crew compartment, and upon inhalation, this energy content is released into the respiratory system as the steam condenses. As a consequence, the temperature of inhaled steam required to cause life-threatening respiratory injury is significantly less than the temperature of dry air. As an example, studies conducted in the 1940s investigating thermal inhalation injuries in dogs found that inhalation of several breaths of steam at a temperature of 100 °C into the pharynx resulted in death owing to obstructive asphyxia [8]. Heuristics have been reported that suggest exposure to a saturated air environment above 70 °C for more than a few seconds is likely to result in severe injury or death [9]. Consequently, a lower escape temperature threshold would need to be used in instances where the moisture content in the crew compartment was high – either owing to the ambient *RH* or the increase in moisture content due to the discharge of water from the suppression system.

The production of HF was confirmed for a number of experiments conducted with the AFESS. No comment can be made about the peak concentrations of HF as measurements were only made after the experiments had been conducted. However, assuming the effective operation of an automatic crew compartment ventilation system, prolonged exposure to high HF levels, if they exist, ought to be minimised.

The AFESS cylinders that utilise nitrogen overpressure as a suppressant delivery mechanism are charged to pressures of the order of 5 MPa and so represent a considerable amount of stored energy should they be struck by an external threat.

The discharge from the extinguisher cylinder could also potentially cause cold temperature burns if discharged next to personnel. A plot of cylinder discharge temperature, as measured with a K-type thermocouple approximately 10 mm downstream of the nozzle is shown in Figure 39.

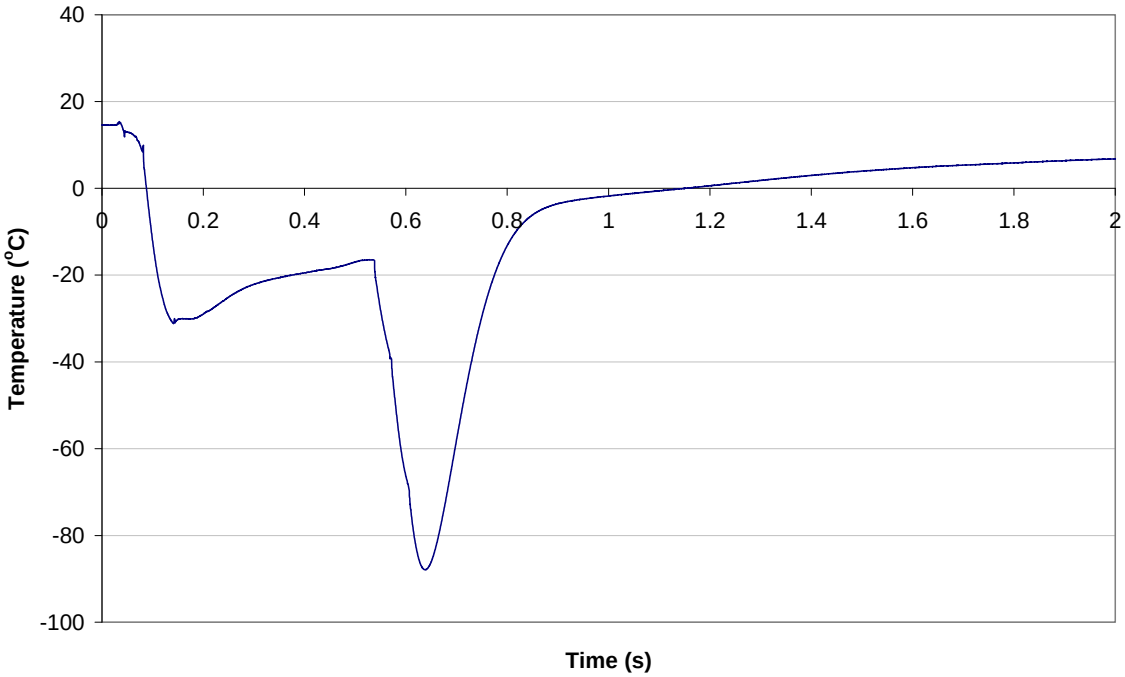

Figure 39: Discharge temperature measured 10 mm downstream of the nozzle for an AFESS gas cylinder without a nozzle

With the exception of the possible exacerbation of superheated steam related threats to the respiratory system if including water in an AFESS, the aforementioned threats can be considered as secondary, and the posed risks are significantly smaller than the risks associated with a propelling charge event in the absence of an AFESS.

5.5 Protective Curtains

A study has been undertaken at the Army Research Laboratory, Aberdeen Proving Ground, to assess the effectiveness of a suite of protective curtain materials protecting stored munitions from fragment and thermal threats [24]. The materials were both inorganic and organic, with a range of thicknesses and weave structures and were subjected to a number of ballistic and thermal threats.

Inorganic (ceramic) layered fabrics conferred thermal protection and Kevlar layers were effective at protecting the stored munitions from low velocity fragments. From the tests conducted, the best protection from both thermal and fragment threats were achieved with a blanket comprised of: four layers of Kevlar 29 Style #745 (0.64 mm ply thickness); two layers of ceramic fabric (0.64 mm ply thickness); and one layer of ceramic felt (3.18 mm ply thickness), all layered inside a Cordura® cover.

Of particular interest in the study was a test where 4x155 mm modular propelling charges were ignited in a horizontally mounted steel tube, sealed at one end, and positioned with a

1m standoff distance from a protective blanket so that the propelling charge fire would impinge directly on the blanket. The back of the blanket was instrumented with thermocouples so that the level of thermal protection afforded to any protected munitions could be quantified.

The propelling charge modules were stated to have produced a high velocity gas and flame impingement on the blanket for a little over one minute [24,25]. Despite this severe thermal insult, complete burn through of the blanket did not occur. With the exception of one thermocouple measurement where flame migration through a seam in the blanket caused a localised temperature at the back of the blanket of 600°C approximately 60 s after charge ignition, there were no other areas where a significant increase in back-surface temperature occurred. Ballistic testing of the same blanket material showed that it was effective at halting a 454 g rectangular fragment travelling at a velocity of 60 m/s without blanket penetration.

The specific weight of the blanket was 4.25 kg/m^2 with a calculated cost, in $US year 2000, of $67 /m^2.

Based on the above results, a properly designed curtain offers the potential to significantly reduce the likelihood of ejecta damage to crew personnel and also prevent initial flame impingement on the crew. If integrated into the platform, in concert with an AFESS designed with due consideration given to the presence of the protective curtains, the crew could be afforded a substantial increase in time before life-threatening thermal injuries are sustained.

6. Trial Limitations

Part 1 of this report [1] addresses a series of limitations associated with the trial that need to be borne in mind when considering the implications of the results presented. In addition to the limitations described in [1], the following points, specific to the hazard mitigation strategies assessed in this report, have relevance to the conclusions stemming from this trial.

6.1 AFESS

The trials design represented the best possible scenario for effective fire suppression. Reasons include:

- The absence of clutter in the trials structure increases the uniformity of suppressant dispersion and increases the rate at which the suppressant is able to reach the source of the fire.
- The suppressant quantity used was based on the uncluttered volume of the crew compartment. Hence, in the presence of representative clutter, the reduced effective crew compartment volume would result in a smaller quantity of suppressant being used. For effective suppressant dispersion, clutter would also likely require the use of a larger number of smaller extinguisher cylinders.

Any further assessment of AFESS effectiveness should be conducted in a trials structure with a representative internal geometry so that the effects of: a reduced internal volume; increased clutter; and, a more realistic extinguisher cylinder distribution, likely consisting of a greater number of smaller cylinders, can be investigated.

In the optimisation of the AFESS design it must be remembered that one of the key functional performance requirements of the system is to extinguish and then prevent re-ignition of fuel-fires. Hence, the AFESS must be designed with due consideration being given to both the fuel-fire and the propelling charge fire threat.

6.2 Clothing

A comparative assessment of the thermal protection afforded by the clothing configurations used in this trial demonstrated the potential thermal protection benefits that could be gained through the judicious selection of clothing. As such, should different clothing configurations to that described in this trial be used, the energy absorption levels of the skin will be affected, thus potentially changing the reported skin burn damage predictions.

7. Conclusions

In a propelling charge initiation event involving a single storage tube inside the crew compartment, the thermal and ejecta threats pose the greatest risk to crew survival.

In the absence of a fire suppression system, a propelling charge event in the crew compartment will create a thermal environment that will cause life-threatening respiratory and skin burn damage with a minimal probability of survival, irrespective of module configuration or ignition location. The sustained, high temperature environment will also pose a sympathetic cook-off risk to other munitions stored within the crew compartment.

As propellant contains both oxygen and fuel required for combustion, the AFESS effectiveness relies on physical suppression via heat absorption. By absorbing heat, the AFESS alters the crew compartment temperature-time profile and under certain conditions this can:

- Reduce the average rate of energy release by delaying the ignition of unburnt propellant
- Reduce the total energy release by preventing the ignition of unburnt propellant

Under certain conditions the above factors, coupled with the energy absorption afforded by the cold temperature discharge of the AFESS suppressant, can increase the time taken before personnel incur a given level of burn damage, thus affording the crew a longer time to escape the platform. For the same reasons, the AFESS can reduce the likelihood of sympathetic cook-off of other munitions in the crew compartment.

The AFESS was least effective against the more dynamic 3xBCM events and its effectiveness also appears to be strongly influenced by initial charge ignition development prior to AFESS discharge. Spatial parameters, such as the distribution of ejected propellant relative to the extinguishers, will also likely influence the AFESS effectiveness.

An AFESS test conducted with the use of water extinguishers in addition to the gas extinguishers proved more effective at suppressing the crew compartment temperature and quantity of burnt propellant than gas extinguishers alone. However, as the nozzle configuration in the two experiments conducted to investigate the effect of water were not identical, it is not possible to determine the relative contribution of the water and the more directed gas discharge on the observed benefits. It should also be noted that an increasing level of moisture in the crew compartment will reduce the maximum survivable temperature and this should be considered when evaluating the benefits afforded by an AFESS that utilises water.

If not damaged by ejecta, the use of Nomex reduces thermal energy absorption by the skin after 10 s by approximately 30%. Wearing cotton below the Nomex results in an 80% reduction in 10 s energy absorption level relative to exposed skin. Consequently, the judicious selection of clothing (material, thickness, number of layers) can be used to afford increased thermal protection from skin burns.

Ejecta in the form of unburnt propellant grains and/or propelling charge modules pose a life threatening risk to crew for all baseline tests conducted [1]. Ejecta damage to personnel may be reduced by weakening the storage tube end-cap seal, other benefits of such a modification may include:

- Enhanced AFESS effectiveness
- Reduced propellant grain fragmentation and subsequent rate of energy release
- Reduced likelihood of storage tube fragmentation
- Reduced effect of tube depressurisation on crew compartment pressure

Whilst not assessed in the trial, the use of fragment and thermally resistant curtains to cover the propelling charge storage tubes in the crew-compartment may enhance the likelihood of crew survival from a thermal and ejecta perspective. If incorporated into a platform as a hazard mitigation strategy, the presence of the curtains would need to be considered when designing the configuration of the crew compartment AFESS.

The generation of HF as a result of high temperature decomposition of the fluorocarbon-based suppressant used in the AFESS was observed. Whilst real-time measurements of the chemical composition of the crew compartment were not made during the trial, oxygen dilution and the presence of toxic propellant combustion species such as CO and CO_2 would occur as a result of the propelling charge event. However, such risks were considered secondary to the immediately life-threatening hazards associated with the thermal and ejecta environments in the crew compartment.

Results and observations from this work suggest that the effective integration and optimisation of one or more of the aforementioned hazard mitigation strategies would likely

increase the chances of crew survival when exposed to the stimuli from a single storage tube propelling charge event.

8. Recommendations

This work allowed the key threats posed to crew personnel and the effectiveness of a range of hazard mitigation strategies, in a propelling charge fire, to be identified.

Conducting a second trial, with an accurate representation of the clutter in the crew compartment, and with the crew compartment in its correct orientation, would allow a more representative assessment of the following hazard mitigation strategies and would permit the resolution of the points below:

AFESS

- Effectiveness in a more representative, challenging environment.
- Repeatability of water effectiveness and discrimination of the benefits afforded by the water and the more directed gas discharge.
- Effectiveness of the water containing AFESS against the worst, and most probable, initiation scenario of 3xBCM (or 3xATC) modules.

Storage tube end-cap sealing strength reduction

- To what extent does this modification enhance the effectiveness of the AFESS?
- Allow the effect of reduced tube confinement on the quantity and velocity of ejecta to be assessed.
- Allow the effect of reduced tube confinement, and therefore reduced rate of tube depressurisation, on propellant extinguishment to be investigated.

Protective curtains could also be considered for assessment in a second trial. Their inclusion could enhance the likelihood of crew survival, but would need to be considered when designing the AFESS and with due consideration to operational logistics in the crew compartment.

If conducted, a second trial should focus on the more dynamic 3xBCM and also the 3xATC configurations.

9. Acknowledgements

The authors are indebted to the following people and organisations, all of whom contributed greatly to the successful completion of this work program:

CAPT Mathew Brooks, JPEU Pt Wakefield, for facilitating the many non-routine activities conducted over the course of the trial and for his willingness to go above and beyond the call of duty to help ensure that maximum benefit was gained from the trial.

Mr Ian Argent, JPEU Pt Wakefield, for his excellent audio visual support, and preparedness to accommodate varying requirements as the trial progressed.

Pacific Scientific HTL-KinTech Divison for provision of the AFESS, including extinguishers, optical detectors and nozzles. Mr Tony Dos Santos and Mr Jesus Acosta, also of Pacific Scientific, for travelling to Australia to install and operate the system during the trial. Mr Stephen Ralph of Cambridge Technologies, in conjunction with Mr Robin Squires of Pacific Scientific, for facilitating the collaborative program with Pacific Scientific, and for the customised design and provision of AFESS cabling and mounting brackets. Without the generous support of these two organisations, the inclusion of the AFESS testing in the trial would not have been possible.

Mr Gordon Proctor and Mr Michael Footner for instrumentation and data acquisition support and Mr Shaun McCormack for hi-speed camera support.

Mr Alan Starks and Mr Roger Cockerill for undertaking the transportation of energetic materials and hardware throughout the course of the trial.

10. References

1 Hart, A.H., Lade, B., Hale, G., (2013), *Survivability of a Propellant Fire inside a Simulated Military Vehicle Crew Compartment: Part 1 – Baseline Study*, **DSTO-RR-0392**, Weapons and Countermeasures Division – DSTO Edinburgh.

2 Hart, A.H., (2013), *Automatic Fire Suppression Systems for Armoured Vehicles: A Review*, **DSTO Technical Report**, Weapons and Countermeasures Division – DSTO Edinburgh, in preparation.

3 Torvi, D.A., Dale, J.D., (1994), *A Finite Element Model of Skin Subjected to a Flash Fire*, **Journal of Biomechanical Engineering**, 116, pp. 250-255.

4 Gasperin, M., Juricic, D., Musizza, B., Mekjavuc, I., (2008), *A Model-Based approach to the Evaluation of Flame-Protective Garments*, **ISA Transactions**, 47, pp. 198-210.

5 **ISO 13506**, (2008), *Protective clothing against heat and flame – Test Methods for complete garments – Prediction of burn injury using an instrumented manikin*.

6 Henriques, F.C., Jr., Moritz, A.R., (1947), *Studies of Thermal Injuries V. The Predictability and the Significance of Thermally Induced Rate Processes Leading to Irreversible Epidermal Injury*, **Archives of Pathology**, 43, pp. 489-502.

7Pryor, A.J., (1968), *Full-Scale Evaluation of the Fire Hazard of Interior Wall Finishes*, Southwest Research Institute, San Antonio. As cited in Bryan, J.L., (1986), **Fire Safety Journal**, 11, pp. 15-31.

8 Moritz, A.R., Henriques, F.C., McLean, R., (1945), *The Effects of Inhaled Heat on the Air Passages and Lungs*, **American Journal of Pathology**, 21, pp. 311-331.

9 Garner, R.P., (1994), *The Potential for Pulmonary Heat Injury Resulting from the Activation of a Cabin Water Spray System to Fight Aircraft Cabin Fires*, **DOT/FAA/AM-94/X**, FAA Civil Aeromedical Institute.

10 Axelsson, H., Yelverton, J.T., (1996), *Chest Wall Velocity as a Predictor of Nonauditory Blast Injury in a Complex Wave Environment*, **The Journal of Trauma: Injury, Infection and Critical Care**, 40(3), pp. S31-S37.

11 Clare, V.R. et al, (1975), *Blunt Trauma Data Correlation*, **Edgewood Arsenal report AD-A012 761**, Figure 7, pg 21.

12 MSDS, (28 Feb 2008), FM200, CAS Number 431-89-0, DuPont.

13 Skaggs, S.R., Moore, T.A, Tapscott, R.E., (1995), *Toxicological Properties of Halon Substitutes*, **Halon Replacements**, ACS Symposium Series, 611, pp. 99-109.

14 Skaggs, R.R., (2002), *Assessment of the Fire Suppression Mechanics for HFC-227ea combined with $NaHCO_3$.*, **12th Halon Options Technical Working Conference**, Albuquerque, New Mexico.

15 Personal communication, Mr Tony Dos Santos and Mr Jesus Acosta, Pacific Scientific HTL Kin-Tech Division, 29/6/10.

16 Williams, B.A., L'Esperance, D.M., Fleming, J.W., (2000), *Intermediate Species Profiles in Low-Pressure Methane/Oxygen Flames Inhibited by 2-H Heptafluoropropane: Comparison of Experimental Data with Kinetic Modelling*, **Combustion and Flame**, 120, pp. 160-172.

17 McCormick S., Clauson, M., (2006), *Halon Replacment Program (HRP) for US Army Ground Combat Vehicles*, **TACOM TARDEC Report Number 15837 RC**.

18 Personal communication, Ms Kit Cassidy, Combat Clothing Sustainment Technical Manager, Defence Materiel Organisation, 25/5/10.

19 Stoll, A.M., Greene, L.C., (1959), **Journal of Applied Physiology**, 14, pp.373-382. As cited in [3].

20 NATO Report: **RTO-TR-HFM-090**, *Test Methodology for Protection of Vehicle Occupants against Anti-Vehicular Landmine Effects*, April 2007, Chapter 3-4.

21 Detail Specification: Valve and Cylinder Assemblies, Halon 1301, (30 Sept 1998), **MIL-DTL-62547C(AT)**.

22 Wierenga, P.H., (2001), *Advanced Environmentally Friendly Fire Protection Technology,* **Halon Options Technical Working Conference**, pp. 373-388.

23 Kim, A., Liu, Z., Crampton, G., (2004), *Explosion Suppression of an Armoured Vehicle Crew Compartment*, National Research Council Canada Report, **NRCC-47026**.

24 Chin, W.K., Mulkern, T.J., Tewarson, A., (2000), *Fire-Resistant and Fragment Penetration-Resistant Blankets for the Protection of Stored Ammunition*, **ARL-TR-2285**.

25 Email communication, Wai K. Chin, Army Research Laboratory, Aberdeen Proving Ground, Maryland, US, 15/6/12.

Appendix A: Test Condition Summary

Table 17: Crew compartment environmental conditions prior to conduct of experiments

Experiment	Date	$T_{ambient}$ (°C)	*RH* (%)
1	23/6/10	17	61
2	24/6/10	10.5	81
3	25/6/10	14.5	72
4	29/6/10	9	93
5	29/6/10	14	78
6	30/6/10	14	78
7	1/7/10	17	52
8	2/7/10	19.5	67
9	5/7/10	16	46
10	6/7/10	12	76
11	6/7/10	18.5	50
12	6/7/10	17	52
13	7/7/10	18	53
14	8/7/10	18	45
15	8/7/10	19.5	44

Table 18: AFESS extinguisher details

Experiment	Serial #	Mass before (kg)	Mass after (kg)	Discharge mass (kg)
5	12744	12.69	7.5	5.19
	12743	12.3	7.26	5.04
	12753	12.61	7.66	4.95
	12734	12.57	7.6	4.97
6	12755	12.63	7.7	4.93
	12746	12.68	7.69	4.99
	12736	12.48	7.53	4.95
	12745	12.66	7.58	5.08
7	12733	12.56	7.57	4.99
	12750	12.62	7.65	4.97
	12747	12.63	7.71	4.92
	12732	12.38	7.45	4.93
8	12754	12.62	7.64	4.98
	12735	12.7	7.5	5.2
	12742	12.67	7.6	5.07
	12751	12.6	7.7	4.9
13	12740	12.67	7.68	4.99
	12752	12.63	7.65	4.98
	12741	12.68	7.65	5.03
	12739	12.35	7.34	5.01
	12755(water)	11.23	7.8	3.43
	12746(water)	10.8	7.79	3.01

Appendix B: Hydrogen Fluoride Protection Measures

The presence of HF inside the simulated crew compartment post-AFESS experiments was noted during a number of experiments, see for example photographs of Drager tubes showing the presence of HF (as indicated by yellow discolouration) in concentrations of 15 ppm and 5 ppm after Experiment 6.

Figure 40: Drager tubes showing the presence of HF inside the trials structure after Experiment 6.

After conducting a test with the AFESS, personnel were only permitted to approach the trials structure wearing specific personal protective equipment (PPE) which was comprised of:

- Tychem disposable impervious coveralls
- Viton/Butyl full length gloves
- Rubber boots
- Chemically resistant full-face respirator fitted with type B inorganic and acid gas canisters

Prior to entering the trials structure, a Drager pump fitted with HF selective tubes was used to measure the concentration of HF. Measurements were made through the two access doors and were sampled from the head-space of the structure as the HF will accumulate at the ceiling due to its lower density relative to air.

An entry HF threshold concentration of 3 ppm or less was set in accordance with the Australian Safety and Compensation Council's time-weighted average exposure level for an 8 hour working day, 5 day working week without experiencing any adverse health effects. It is noted that this is a very conservative threshold given the level of PPE worn by the staff undertaking the decontamination process and the limited exposure time in the affected environment (typically less than 1 hour during the trials structure decontamination procedure).

Once the entry threshold criteria was satisfied, any unburnt propellant or debris was placed in buckets filled with an emulsion of calcium carbonate and water to neutralise any HF that may have condensed on their surfaces. The inside surfaces of the structure were then dusted down with calcium carbonate using a broom. The surfaces were then mopped down with an emulsion of calcium carbonate and water before being left to dry, see Figure 41.

Figure 41: Mopping down of the trials structure with calcium carbonate/water emulsion after preliminary dusting with calcium carbonate

After decontamination of the trials structure, any used equipment such as mops and brooms were rinsed with a calcium carbonate/water emulsion to neutralise any residual HF that may have been transferred during the decontamination process.

Personnel were decontaminated using a staged decontamination shower system that first involved mopping down the protective clothing with a calcium carbonate/water emulsion, Figure 42, and then entering the decontamination shower, see Figure 43.

Figure 42: Preliminary decontamination of staff with calcium carbonate/water emulsion

Figure 43: Shower decontamination

As an additional precaution, all staff involved in the decontamination of the trials structure were provided with tubes of calcium gluconate gel to treat any HF burns in the unlikely event that they occurred. Range medics, trained in the administration of calcium gluconate injections, were also on call in the event of a more serious HF burn event.

DEFENCE SCIENCE AND TECHNOLOGY ORGANISATION
DOCUMENT CONTROL DATA

1. PRIVACY MARKING/CAVEAT (OF DOCUMENT)

2. TITLE

Survivability of a Propellant Fire inside a Simulated Military Vehicle Crew Compartment: Part 2 - Hazard Mitigation Strategies and Their Effectiveness

3. SECURITY CLASSIFICATION (FOR UNCLASSIFIED REPORTS THAT ARE LIMITED RELEASE USE (L) NEXT TO DOCUMENT CLASSIFICATION)

Document	(U)
Title	(U)
Abstract	(U)

4. AUTHOR(S)

Andrew H. Hart, Blair C. Lade and Garry R. Hale

5. CORPORATE AUTHOR

DSTO Defence Science and Technology Organisation
PO Box 1500
Edinburgh South Australia 5111 Australia

6a. DSTO NUMBER	6b. AR NUMBER	6c. TYPE OF REPORT	7. DOCUMENT DATE
DSTO-RR-0393	AR-015-621	Research Report	June 2013

8. FILE NUMBER	9. TASK NUMBER	10. TASK SPONSOR	11. NO. OF PAGES	12. NO. OF REFERENCES
2012/1016134/1	CDG 09/0007	CDG	77	25

13. DSTO Publications Repository

http://dspace.dsto.defence.gov.au/dspace/

14. RELEASE AUTHORITY

Chief, Weapons and Countermeasures Division

15. SECONDARY RELEASE STATEMENT OF THIS DOCUMENT

Approved for public release

OVERSEAS ENQUIRIES OUTSIDE STATED LIMITATIONS SHOULD BE REFERRED THROUGH DOCUMENT EXCHANGE, PO BOX 1500, EDINBURGH, SA 5111

16. DELIBERATE ANNOUNCEMENT

No Limitations

17. CITATION IN OTHER DOCUMENTS Yes

18. DSTO RESEARCH LIBRARY THESAURUS

Hazard analysis, Risk assessment, Risk mitigation, Crew environments, Modelling, Survivability

19. ABSTRACT

A number of combat vehicles carry their propelling charges and high explosive filled projectiles inside the crew compartment. Such arrangements give rise to questions about the prospects of crew survival in an unplanned munitions initiation event owing to co-habitation of the crew with an on-board magazine. DSTO has undertaken an experimental study to investigate this concern. As part of the trial described in Part 1 of this report, the following hazard mitigation strategies were assessed for their effectiveness at reducing the thermal, ejecta and pressure threats posed to the crew by a range of propelling charge fire scenarios: two MIL-STD Automatic Fire Suppression configurations; personnel clothing configurations; and propelling charge storage tube confinement modificaton. Results from the study suggest that the prospects of crew survival could be improved by the implementation of one or more of the hazard mitigaton strategies described within.